AD-A055 606 SYBUCON INC ATLANTA GA F/G 20/4

VERIFICATION OF A THREE-DIMENSIONAL TURBULENT BOUNDARY-LAYER CA--ETC(U)

FEB 78 J F NASH, R M SCRUGGS F33615-77-C-3116

UNCLASSIFIED AFFDL-TR-78-15 NL

1 OF 1

AD A055606

END

DATE FILMED

8 -78

DDC

FOR FURTHER TRAN

AFFDL-TR-78-15

(2)

AD A055606

VERIFICATION OF A THREE-DIMENSIONAL TURBULENT BOUNDARY-LAYER CALCULATION METHOD

JOHN F. NASH
ROY M. SCRUGGS
SYBUCON, INC.
1900 THE EXCHANGE, SUITE 175
ATLANTA, GEORGIA 30339

AD No.
DDC FILE COPY

FEBRUARY 1978

TECHNICAL REPORT AFFDL-TR-78-15
Final Report

Approved for public release; distribution unlimited.

AIR FORCE FLIGHT DYNAMICS LABORATORY
AIR FORCE WRIGHT AERONAUTICAL LABORATORIES
AIR FORCE SYSTEMS COMMAND
WRIGHT-PATTERSON AIR FORCE BASE, OHIO 45433

78 06 16 039

NOTICE

This technical report has been reviewed and is approved for publication.

Albert J. Murn

ALBERT J. MURN
Project Engineer

FOR THE COMMANDER

Alfred C. Draper

ALFRED C. DRAPER
Assistant for Research & Technology
Aeromechanics Division

AIR FORCE/56780/1 May 1978 — 250

UNCLASSIFIED

SECURITY CLASSIFICATION OF THIS PAGE (When Data Entered)

18 19 REPORT DOCUMENTATION PAGE

READ INSTRUCTIONS BEFORE COMPLETING FORM

1. REPORT NUMBER: AFFDL-TR-78-15

2. GOVT ACCESSION NO.

3. RECIPIENT'S CATALOG NUMBER

4. TITLE (and Subtitle): 6 VERIFICATION OF A THREE-DIMENSIONAL TURBULENT BOUNDARY-LAYER CALCULATION METHOD

5. TYPE OF REPORT & PERIOD COVERED: 9 Final Technical Report, August 1977 - DEC [redacted]77

6. PERFORMING ORG. REPORT NUMBER

7. AUTHOR(s): 10 John F. Nash [redacted] Roy M. Scruggs

8. CONTRACT OR GRANT NUMBER(s): 15 F33615-77-C-3116

9. PERFORMING ORGANIZATION NAME AND ADDRESS: Sybucon, Inc. 1900 The Exchange, Suite 175 Atlanta, Georgia 30339

10. PROGRAM ELEMENT, PROJECT, TASK AREA & WORK UNIT NUMBERS: Program Element 62201F 16 Project 2404, Task 10 17 Work Unit 22

11. CONTROLLING OFFICE NAME AND ADDRESS: Air Force Flight Dynamics Laboratory/FXM Air Force Systems Command Wright-Patterson Air Force Base, Ohio 45433

12. REPORT DATE: 11 February 1978

13. NUMBER OF PAGES: 57

14. MONITORING AGENCY NAME & ADDRESS (if different from Controlling Office): 12 58 p.

15. SECURITY CLASS. (of this report): UNCLASSIFIED

15a. DECLASSIFICATION/DOWNGRADING SCHEDULE

16. DISTRIBUTION STATEMENT (of this Report)

Approved for public release; distribution unlimited.

17. DISTRIBUTION STATEMENT (of the abstract entered in Block 20, if different from Report)

18. SUPPLEMENTARY NOTES

19. KEY WORDS (Continue on reverse side if necessary and identify by block number)

Turbulence Model
Turbulent Boundary Layers
Three-Dimensional Calculations

20. ABSTRACT (Continue on reverse side if necessary and identify by block number)

The boundary-layer calculation method which forms the subject of this verification study, involves a radically different numerical scheme and geometry-handling scheme than has been employed in earlier methods. This turbulence model based on a still earlier two-dimensional model of Bradshaw et.al., incorporates the empirically modified turbulent kinetic-energy equation together with an assumed relationship between the turbulent intensity and the Reynolds shear stress. → next page

DD FORM 1 JAN 73 1473 EDITION OF 1 NOV 65 IS OBSOLETE

UNCLASSIFIED

SECURITY CLASSIFICATION OF THIS PAGE (When Data Entered)

S/C 392 927

20. Abstract (Continued)

The form of this relationship, and the forms of two other empirical functions of position through the boundary layer (the dissipation length and the diffusion function), have to satisfy certain rather broad theoretical constraints but otherwise must be adjusted, by trial and error, to give the best overall agreement with experiment. The emergence of more recent sets of experimental data has indicated the potential for further improvements of the model. Some of these sets of data include more detailed measurements, particularly of the quantities, than were available when the earlier validation was performed.

The study reported here was far from being extensive: comparisons were made with only two sets of measurements in three-dimensional flows. There is a possibility, on that account, that the proposed modifications to the turbulence model will be biassed. In an attempt to minimize such a bias some supporting comparisons have been made with a few sets of two-dimensional data. The results are fairly convincing, but caution must be exercised in interpreting their generality. Until more complete verification has been undertaken the proposed changes must be regarded as tentative.

FOREWORD

This is the final technical report on the experimental verification of an implicit three dimensional turbulent boundary layer code. This report covers work performed by Sybucon, Inc., Atlanta, Georgia. This work was under the technical direction of Capt. James D. Wilson, Air Force Flight Dynamics Laboratory/FXM, Air Force Systems Command, Wright-Patterson Air Force Base, Ohio. John F. Nash was the program manager and Roy M. Scruggs was the principal investigator.

The work was performed under Contract F33615-77-C-3116, Project 2404, Task 10. The study period included August 1977 to December 1977. The final report was submitted in January 1978.

CONTENTS

SECTION		PAGE
I.	INTRODUCTION	1
II.	DESCRIPTION OF THE TURBULENCE MODEL	3
III.	COMPARISONS WITH EXPERIMENT	6
	° Experimental Test Cases	6
	° Comparison Between the Original Model and Experiment	8
IV.	MODIFICATIONS TO THE MODEL	11
	° Sensitivity to Changes of the Empirical Functions	11
	° History Effect on Dissipation Length	15
	° Proposed Changes to the Turbulence Model	17
	° Comparison Between the Proposed Models and Experiment	19
V.	CONCLUSIONS AND RECOMMENDATIONS	21
	REFERENCES	47

LIST OF ILLUSTRATIONS

Figure		Page
1	Diffusion Function and Dissipation Length	24
2	Comparison with the Data of Klebanoff (Velocity and $\overline{q^2}$ Profiles)	25
3	Comparison with the Data of Ludwieg and Tillmann, and Schubauer and Spangenberg (Wall Shear Stress and Boundary-Layer Thickness)	26
4	Comparison with the Data of Ludwieg and Tillmann (Velocity Profile)	27
5	Comparison with the Data of Schubauer and Spangenberg (Velocity Profile)	28
6	Comparison with the Data of van den Berg and Elsenaar (Wall Shear Stress and Boundary-Layer Thickness)	29
7	Comparison with the Data of van den Berg and Elsenaar (Velocity and $\overline{q^2}$ Profiles at Station #4)	30
8	Comparison with the Data of van den Berg and Elsenaar (Velocity and $\overline{q^2}$ Profiles at Station #7)	31
9	Comparison with the Data of Peake (Wall Shear Stress)	32
10	Comparison with the Data of Peake (Velocity and Temperature Profiles)	33
11	Modifications to Dissipation Length and $f(\psi)$ Considered in the Sensitivity Study	34
12	Effect of Modifications to Dissipation Length	35
13	Effect of Modifications to the Shear-Stress/Turbulent-Kinetic Energy Relationship	36
14	Effect of Representing the Finite Response Time of the Dissipation Length	37

LIST OF ILLUSTRATIONS (Cont'd)

Figure		Page
15	Comparison with the Data of Kelbanoff (Velocity and $\overline{q^2}$ Profiles)	38
16	Comparison with the Data of Ludwieg and Tillmann, and Schubauer and Spangenberg (Wall Shear Stress and Boundary-Layer Thickness)	39
17	Comparison with the Data of Ludwieg and Tillmann (Velocity Profile)	40
18	Comparison with the Data of Schubauer and Spangenberg (Velocity Profile)	41
19	Comparison with the Data of van den Berg and Elsenaar (Wall Shear Stress and Boundary-Layer Thickness)	42
20	Comparison with the Data of van den Berg and Elsenaar (Velocity and $\overline{q^2}$ Profiles at Station #4)	43
21	Comparison with the Data of van den Berg and Elsenaar (Velocity and $\overline{q^2}$ Profiles at Station #7)	44
.22	Comparison with the Data of Peake (Wall Shear Stress)	45
23	Comparison with the Data of Peake (Velocity and Temperature Profiles)	46

LIST OF SYMBOLS

A	Van Driest constant (Equation 2.9)
a_2	Diffusion function
C_f	Skin friction coefficient
C_p	Pressure coefficient
c_p	Specific heat at constant pressure
f, g	Empirical functions (Equations 2.11, 2.12, 2.14)
h_1, h_2, h_3	Metric coefficients corresponding to x, y, z
L_D	Dissipation length
p	Static pressure
Q, q	Resultant mean and fluctuating velocities
$R_{e_{\delta*}}$	Reynolds number based on displacement thickness
T	Static temperature
T_t	Total temperature
U, V, W	Mean velocity components
u, v, w	Fluctuating velocity components
x, y, z	Orthogonal coordinates (with $y = 0$ representing the body surface)
$\hat{y}$	Physical distance normal to the body surface ($= \int_0^y h_2 dy$)
β	Crossflow angle
δ	Boundary-layer thickness
δ_E	Scaling factor for dissipation length (Equation 4.2)
δ^*	Displacement thickness
ε	Dissipation rate
η	Nondimensional distance normal to the body surface ($= \hat{y}/\delta$)

ρ	Density
τ	Shear stress
ϕ	Fluctuating temperature
ψ, ψ_T	Arguments of the functions f, g

Subscripts

e	Value at the edge of the boundary layer
w	Value at the wall

SECTION I. INTRODUCTION

The boundary-layer calculation method [1], which forms the subject of this verification study, was developed by Sybucon under Air Force funding via a subcontractual relationship with Grumman Aerospace Corporation. The method involved a radically different numerical scheme and geometry-handling scheme than had been employed in earlier methods, but essentially the same turbulence model as one that had been in continuous use for several years [2]. This turbulence model, based on a still earlier two-dimensional model of Bradshaw et. al. [3], incorporates the empirically modified turbulent kinetic-energy equation together with an assumed relationship between the turbulent intensity and the Reynolds shear stress.

The form of this relationship, and the forms of two other empirical functions of position through the boundary layer (the dissipation length and the diffusion function), have to satisfy certain rather broad theoretical constraints but otherwise must be adjusted, by trial and error, to give the best overall agreement with experiment. A process of optimization, on these lines, was carried out six to seven years ago [4, 5] and the resulting model has since enjoyed a reputation for good reliability and accuracy. The emergence of more recent sets of experimental data, however, has indicated the potential for further improvements of the model. Some of these sets of data include more detailed measurements, particularly of the turbulence quantities, than were available when the earlier validation was performed. The need for validation of method in compressible flow has also been recognized for some time.

The study reported here was far from being extensive: comparisons were made with only two sets of measurements in three-dimensional flows. There is a possibility, on that account, that the proposed modifications to the turbulence model will be biassed. In an attempt to minimize such a bias some supporting comparisons have been made with a few sets of two-dimensional data. The results are fairly convincing, but caution must be exercised in interpreting their generality. Until more complete verification has been undertaken the proposed changes must be regarded as tentative.

The strategy adopted for verification and fine-tuning of the turbulence model consisted of three steps:

- comparison with experiment, using the existing model
- determination of the sensitivity of the predictions to changes of the empirical functions
- comparison with experiment using various candidate revised models.

Section II reviews the various relationships which define the existing turbulence model, and Section III presents the comparisons between this model and the experimental test cases. The sensitivity study and the proposed modifications to the model are described in Section IV.

SECTION II. DESCRIPTION OF TURBULENCE MODEL

The calculation method involves the simultaneous solution of five governing equations, together with various peripheral relationships:

- two mean-flow momentum equations
- thermal energy equation
- continuity equation
- empirically modified turbulent kinetic-energy equation.

This last equation, which provides closure of the system of mean-flow equations, is written in the form

$$\frac{\rho U}{h_1}\frac{\partial}{\partial x}\left(\frac{\overline{q^2}}{2}\right) + \frac{1}{h_2}\left(\rho V + \overline{\rho' v}\right)\frac{\partial}{\partial y}\left(\frac{\overline{q^2}}{2}\right) + \frac{\rho W}{h_3}\frac{\partial}{\partial z}\left(\frac{\overline{q^2}}{2}\right) +$$

$$\frac{\rho\overline{uv}}{h_2}\frac{\partial U}{\partial y} + \frac{\rho\overline{vw}}{h_2}\frac{\partial W}{\partial y} + \frac{\rho}{h_2}\frac{\partial}{\partial y}\left(\frac{\overline{p'v}}{\rho} + \frac{\overline{q^2 v}}{2}\right) + \rho\varepsilon = 0, \tag{1}$$

where

$$\overline{q^2} = \overline{u^2} + \overline{v^2} + \overline{w^2} . \tag{2}$$

Additional empirical relationships are provided to model the diffusion and dissipation terms, and to model the dependence of the turbulent shear stresses and turbulent heat flux on $\overline{q^2}$.

Specifically, following Bradshaw et al. [3] and Nash [2], the diffusion and dissipation terms are modeled, respectively by

$$\frac{\overline{p'v}}{\rho} + \frac{\overline{q^2 v}}{2} = \frac{\overline{q^2}_{max}}{Q_e}\, a_2\, \overline{q^2} \tag{3}$$

$$\varepsilon = \frac{(q^2)^{3/2}}{L_D} , \tag{4}$$

where q^2_{max} is the maximum value of $\overline{q^2}$ in the outer three-fourths of the boundary-layer, and where the diffusion function: a_2, and the dissipation length: L_D, are assumed to be universal functions of physical distance through the boundary layer. The existing forms for a_2 and L_D, are the same as those found appropriate in earlier studies [4, 5], and can be represented by

$$a_2 = 1.125\ \eta^2 - 0.375\ \eta^4 \tag{5}$$

$$\frac{L_D}{\delta} = \frac{7.195\eta}{1 + 4\eta^2 + 5\eta^7}\ . \tag{6}$$

These two functions are illustrated in Figure 1. In Equations (2.5, 6) η is the dimensionless physical distance through the boundary layer:

$$\eta = \frac{1}{\delta} \int_o^y h_2 dy\ , \tag{7}$$

and δ is the boundary-layer thickness, defined as the distance from the surface where

$$\{(U_e - U)^2 + (W_e - W)^2\}^{\frac{1}{2}} = 0.005\ Q_e. \tag{8}$$

Close to the surface the dissipation length is modified by the Van Driest correction [6]

$$(L_D)_{corr.} = L_D\ (1 - e^{-y^+/A}) \tag{9}$$

where

$$y^+ = \frac{\delta}{\rho}\ (\tau_w)^{\frac{1}{2}}\eta \tag{10}$$

and A is a constant usually taken to be 26.

The turbulent shear-stress components are related to $\overline{q^2}$ by empirical functions of the form

$$\rho\overline{uv} = -\rho\overline{q^2}\ f\left\{\frac{L_D}{(\overline{q^2})^{\frac{1}{2}}h_2}\frac{\partial U}{\partial y}\right\} \tag{11}$$

$$\rho\overline{uw} = -\rho\overline{q^2}\ f\left\{\frac{L_D}{(\overline{q^2})^{\frac{1}{2}}h_2}\frac{\partial W}{\partial y}\right\} \tag{12}$$

In the method of Reference 1 the function f was tentatively assumed to be linear

$$f(\psi) = 0.0225\ \psi, \tag{13}$$

but the intention was to study the implications of using other forms at a later date. Some of these implications are explored below.

The corresponding relationship between turbulent heat flux and $\overline{q^2}$ is written as

$$\overline{v\Phi} = -\frac{(\overline{q^2})^{3/2}}{c_p}\ g\left\{\frac{c_p L_D}{\overline{q^2}h_2}\frac{\partial T}{\partial y}\right\} \tag{14}$$

where g is another empirical function. The method of Reference 1 was based on the provisional form

$$g(\psi_T) = \frac{0.0225}{Pr_t}\psi T \tag{15}$$

in which Pr_t is an assumed constant value (= 0.9) of the turbulent Prandtl number.

SECTION III. COMPARISONS WITH EXPERIMENT

Experimental Test Cases

The sets of experimental data, with which the predictions were compared, are described below.

1. Two-dimensional incompressible flow over a flat plate.

   The classical experiment of Klebanoff [7] provided the main source of data for this test case. Mean-flow data and turbulence measurements are reported in Klebanoff's paper. The mean-flow measurements of Smith and Walker [8] and empirical correlations proposed by Rotta [9] and Coles [10], provided additional data.

2. Two-dimensional incompressible flow in an adverse pressure gradient.

   Two sets of data were selected to represent this type of flow: the measurements of Ludwieg and Tillman [11] in a strong adverse pressure gradient, and the measurements of Schubauer and Spangenberg, "Flow A" [12]. These two sets of data were designated Numbers 1200 and 4400, respectively, in Stanford Conference proceedings [13]. Mean-flow measurements, only are given in these references.

3. Three-dimensional incompressible flow over a swept wing. The mean-flow data of van den Berg and Elsenaar [14], and the turbulence measurements of Elsenaar and Boelsma [15] (which were made on the same wing model) formed the input to this principal test case. The measurements, which were made in the Netherlands, were designed to closely simulate infinite-swept wing conditions. The small residual variations in the spanwise direction were accounted for in the calculations. Interesting background information, pertaining to the present study is provided by the attempts of other investigators to match the van den Berg-Elsenaar data; these attempts are reported in Reference 16.

4. Three-dimensional supersonic flow through a swept shock. The data of Peake [17] were used for this second principal test case. The experimental arrangement consisted of a shock generator standing normal to a flat plate. The shock formed by the generator interacted with the boundary layer developing on the plate. The measurements were made in this region of interaction where the flow suffered a strong lateral perturbation. Two sets of data are reported in Peake's paper; the one at a Mach number of 2 was selected for comparison purposes because boundary-layer separation was not provoked by the interaction. Separation did occur in the other set of data, at M = 4.

Comparison Between the Original Model and Experiment

The comparisons between predictions, using the original turbulence model, and experiment are presented in Figures 2 through 10. For the two-dimensional flat-plate flow (Figure 2) the calculation is in good agreement with the measured velocity and turbulent-kinetic-energy profiles. However, the wall shear stress is underpredicted: C_f is predicted to be 0.00256, compared to the measured value of 0.0028. The discrepancy is associated with the failure of the method to recover the precisely appropriate additive constant in the logarithmic wall law; it was noted in Reference 1 that the predicted additive constant is about 2.5 compared with Patel's experimental value of 2.3.

For two-dimensional flow in an adverse pressure gradient (Figures 3 through 5) there is a tendency for the velocity to be overpredicted in the inner half of the boundary layer -- the shape of the velocity profile does not respond sufficiently to the effects of the pressure gradient. On this basis one would presume that the predicted separation point would lie too far downstream. On the other hand, for at least one of the cases: Schubauer and Spangenberg (Figure 3), the predicted variation of C_f with x is of the right form (even though the values are somewhat low).

The calculated flow over the swept wing was matched at x/c = 0.34 (denoted "measuring station #1" in Reference 14), and good agreement between theory and experiment is obtained over the early part of the run (Figure 6), except for the underprediction of C_f which occurs in most of the comparisons. At x/c = 0.54 (station #4), Figure 7 shows that the predicted vector velocity profile is in excellent agreement with measurement, and that the predicted $\overline{q^2}$ profile agrees with the measured one to within the probable level of experimental accuracy. Further downstream, however, the agreement between theory and experiment is less good; in fact the agreement deteriorates in the same manner as other investigators have found (see Reference 16). Figure 8, which corresponds to x/c = 0.74 (station #7), shows the familiar overprediction of resultant velocity, underprediction of crossflow angle, and underprediction of boundary-layer thickness. Interestingly, the turbulent-kinetic-energy profile is predicted quite well. Separation, defined in this instance as the condition where the limiting streamlines lie parallel to the sweep lines, was observed to occur experimentally at about x/c = 0.87. The calculation, however, continued to the trailing edge without anywhere reaching that level of wall streamline deflection.

The calculation for the supersonic swept-shock flow was adjusted to give the appropriate constant-pressure profile at about x = -1.in., where x is measured from the position of the inviscid shock front. At this condition, the predicted skin-friction coefficient lies close to the experimental value given by a circular Preston tube. The latter value lies above the measurement made by the NAE cobra probe, but below the value derived from the Spalding/Chi correlation [19] for two-dimensional constant-pressure boundary layers (Figure 9). The predicted subsequent decrease of C_f, resulting from the shock interaction, follows a trend which is consistent with the experimental data. However, the appreciable scatter of the data -- and more particularly the discrepancy between the measurements made using the two different devices -- precludes any detailed comment about the accuracy of the predictions. The wall streamline deflection angle (measured, here, relative to the tunnel center line) is shown in the lower part of Figure 9. The prediction of this quantity was found to depend rather critically on the assumed conditions along the edge of the integration domain nearest to the shock generator. The effect of these conditions, on the solution at the center line, conformed with the requirements of the appropriate zones of influence but was still appreciable. The solution shown in Figure 9 corresponds to a conservative assumption about the edge conditions, and indicates an underprediction of the deflection angle on the center line.

The predicted crossflow angle through the boundary layer (measured relative to the external streamlines) is in good agreement with experiments except close to the wall (Figure 10). The comparison is for $x = 0$, which is three-fourths the way up the pressure rise. The resultant velocity is overpredicted for reasons which are associated with the underprediction of streamline deflection angle. The predicted total-temperature profile agrees with the measured one to within 2-3%; the only significant discrepancy appears to be an exaggeration (in the calculation) of the variations above and below the free-stream total temperature. The predicted and measured wall temperatures are in close agreement.

SECTION IV. MODIFICATIONS TO THE MODEL

Sensitivity to Changes of the Empirical Functions

The turbulence model involves four distinct empirical functions which are relevant in incompressible flow:

- the diffusion function (Equation 2.5)
- the dissipation length (Equation 2.6)
- the Van Driest correction to dissipation length in the wall region (Equation 2.9)
- the relationship between shear stress and turbulent kinetic energy (Equations 2.11 and 2.12)

It has previously been shown [3] that the form of the diffusion function has relatively little effect on the solutions and, for this reason, it was left unchanged during the present studies. Effort was directed to exploring the effects of modifying the other empirical functions. Most of these sensitivity studies were carried out using incompressible flat-plate flow as a test case. Specifically, the following modifications were tried, one at a time:

(a) changing the constant in the numerator of the dissipation length function (Equation 2.6) to 6.143, which reduces the values of L_D throughout the boundary layer

(b) changing the denominator of the dissipation length function to

$$1 = 5\eta^2 + 14\eta^7,$$

which reduces the values of L_D over the central and outer parts of the boundary layer

(c) changing the denominator of the dissipation length function to

$$1 + 5\eta^2 + \eta^7$$

which increases the values of L_D over the outer part of the boundary layer

(d) changing the value of A in the Van Driest formula to 13, which reduces the thickness of the viscous sub-layer

(e) increasing the constant in Equation (2.13) to 0.0278, which increases the shear stress for a given level of turbulent intensity

(f) modifying the form of the relationship between shear stress and turbulent intensity by imposing a ceiling of 0.15 on the value of f

(g) increasing the constant in Equation (2.13) to 0.0278 and also imposing a ceiling of 0.167 on the value of f.

These changes are illustrated in Figure 12. In modifications (f) and (g) the break points between the two line segments, defining the function, were arranged to lie on the hyperbola $f = 1/\psi$ which, for two-dimensional flow, corresponds to the statement "production = dissipation". The desirability of imposing the ceiling on the value of f was suggested partly by experimental data and, more strongly, by conceptual arguments that the value of f ought to reach a maximum for large rates of strain -- or even to decrease for large total strains [17]. A difficulty arises, however, that any departure from a proportionality relationship between f and ψ implies that the resulting model is not invariant to rotation of the coordinate axes. There are ways of surmounting this difficulty, by redefining the parameters involved, but they were not considered here because significant coding changes would have been required. The results obtained from modifications (f) and (g), above, therefore have to be evaluated in terms of the particular coordinate system used here (parallel and normal to the undistrubed flow at infinity).

The results of the sensitivity study are shown in Figures 12 through 14. Here the predicted velocity profiles, and profiles of $\overline{q^2}$, are compared for a Reynolds number of 10^4 based on displacement thickness. The main observation is that none of the changes has more than a minimal effect on the velocity profile, but some of them have a pronounced effect on turbulent kinetic energy. The effect on turbulent kinetic energy is surprisingly large in the case of the modification to the Van Driest constant. It might be thought that this constant would only affect conditions in the sublayer; however, it emerges that the effect is distributed across the whole boundary layer. The interpretation is that the level of $\overline{q^2}$ at the edge of the sublayer through which the variation of $\overline{q^2}$ is rapid serves as a boundary condition for the solution throughout the fully turbulent region where $\partial\overline{q^2}/\partial y$ is relatively small.

In addition to the results presented in Figures 12 through 14, the following effects of the modifications on wall shear stress were observed (these are all for a value of $R_{e_{\delta^*}} = 10^4$):

Modification	C_f
(a)	0.00212
(b)	0.00244
(c)	0.00248
(d)	0.00296
(e)	0.00298
(f)	0.00234
(g)	0.00270

These values may be compared with 0.00256, obtained using the original model, and with 0.0028 which is Klebanoff's measured value.

The changes to the empirical functions, considered so far, have been evaluated in terms of their effects in incompressible flow. No separate sensitivity study has been conducted under conditions of compressibility. One of the underlying assumptions is that the turbulence model remains valid until the Mach number based on $(\overline{q^2})^{\frac{1}{2}}$ becomes comparable with unity, and that is unlikely to occur below a free-stream Mach number of about 3. The only empirical function that must be studied in a context of compressible flow is the relationship: $g(\psi_T)$, between turbulent heat flux and turbulent kinetic energy (Equation 2.14). A few calculations were done in which a ceiling was imposed on the value of g, by analogy with modifications (f) and (g), above. The results indicated that such a change was inadmissible because it destroyed the conservation of total enthalpy in the boundary layer: the <u>average</u> total temperature was found to exceed the free-stream value. The only modification, made to the relationship in the present work, was to change the constant in the numerator of Equation (2.15): i.e. 0.0225, to 0.0278 whenever the latter value was used in Equation (2.13). In this way the assumed value of the turbulent Prandtl number was preserved, at least for small values of ψ, regardless of the form chosen for $f(\psi)$.

History Effect on Dissipation Length

In addition to the modifications considered above, some studies were made to explore the effects of uncoupling the dissipation length from the local boundary-layer thickness. There are strong conceptual arguments, and some experimental evidence suggesting that the scale of the large eddies, which determines the dissipation length, responds relatively slowly to changes of boundary-layer thickness. The assumption, in the original model, that this response is immediate, leads to an overestimate of dissipation length in boundary layers (such as that of van den Berg, et. al. [14, 15]) which are characterized by large spatial rates of growth.

In order to reflect the finite rate of response of the dissipation length, it is necessary to incorporate a second turbulence equation. Some suggestions are given in Reference 18 as to the appropriate form of such an equation*, but here the global effect is represented simply by replacing δ, in Equation (2.6), by δ_E and by redefining η (in the same equation) as

$$\eta = \frac{1}{\delta_E} \int_0^y h_2 dy \tag{16}$$

where δ_E is an effective thickness which lags behind the physical thickness, δ, according to the rate equation

$$U_e \frac{\partial \delta_E}{\partial x} + W_e \frac{\partial \delta_E}{\partial z} = \frac{Q_e}{k\delta} (\delta - \delta_e). \tag{15}$$

The rate constant, k, is taken provisionally to be 6, implying that the

---

* Other investigators have proposed appropriate forms of an equation for dissipation rate.

dissipation length in the outer part of the layer has a characteristic response time equal to the time taken for a fluid particle to travel a distance of 6δ. In the inner part of the boundary layer the characteristic time becomes shorter, and it reaches zero at the wall. The form of Equation (2.6), with η now given by Equation (4.1), ensures a qualitatively correct variation of the characteristic time across the boundary layer.

Proposed Changes to the Turbulence Model

The most significant weakness of the original model appears to lie in its lack of responsiveness to adverse pressure gradients leading to separation. The simplest means of correcting this weakness is to modify the relationship between shear stress and turbulent kinetic energy. Imposing a ceiling on the value of f (Equations 2.11 and 2.12) prevents the generation of the high shear-stress levels which, in large measure, cause the unresponsiveness. Modification (f), defined above provides a satisfactory provisional improvement although, as noted earlier, it suffers from lack of invariance to rotation of the coordinate system. It also suffers from the deficiency of producing wall shear-stress values which typically are too low. For the flat-plate flow (Section III, above) it was noted that C_f lay about 16% below the experimental value, for $R_{e_{\delta^*}} = 10^4$. This modification will be referred to as "Proposed Model A" in what follows.

An attempt has been made to derive a second model which would exhibit the proper degree of responsiveness, while also producing the correct level of wall shear stress. Considerably more effort was put into the derivation of this model: denoted "Proposed Model B", and it seems to give satisfactory agreement with all the cases considered. Model B reflects the following combination of changes to the empirical functions:

- Modification of the dissipation length function (modification (c) of Section IV, above)
- Modification of the shear-stress/turbulent-kinetic-energy relationship (modification (g) of Section IV)
- Incorporation of the history effect on dissipation length via Equation (4.2)

The proposed modification to the dissipation length (Figure 11) has the effect of increasing the levels of $\overline{q^2}$ and shear stress in the outer part of the boundary layer. This is desirable, for flows in small adverse pressure gradients, to offset the decrease brought about by allowing the dissipation length to lag behind the local boundary-layer thickness. For flows in severe adverse pressure gradients the two effect do not offset one another and the proper reduction in shear stress is achieved. The modification to the f-function (Figure 11) further limits the growth of turbulent kinetic energy in strong adverse pressure gradients. However, the higher slope of the function, for small values of the argument, improves the flat-plate solution and results in more accurate wall shear-stress predictions. It was not found desirable to change the Van Driest constant; nor, as mentioned earlier, have any possible modifications to the diffusion function been explored.

Comparison Between the Proposed Models and Experiment

Calculations involving the Proposed Models A and B are compared with the original calculations, and with the experimental data, in Figures 15 through 23.

For two-dimensional flow over a flat plate there was little room for improvement as far as the profiles of velocity and $\overline{q^2}$ are concerned. Figure 15 shows that agreement with the measured velocity profile may perhaps be slightly better with the new models, whereas agreement with $\overline{q^2}$ is slightly worse (if the measurements are sufficiently accurate to make such a judgment). The associated wall shear-stress values, for a Reynolds number of 10^4 based on displacement thickness, are as follows:

Model	C_f
Original Model	0.00256
Proposed Model A	0.00234
Proposed Model B	0.00272
Experiment (Klebanoff)	0.0028
Experiment (Smith & Walker)	0.0027

There is some evidence that the error in C_f for Model A results partly from truncation errors in the solution method, and is substantially reduced when the calculation is done to second-order accuracy. It should be recognized that the fine-tuning of the turbulence model, attempted here, may have been hampered by numerical errors (although these are believed generally to be small). Furthermore, the possibility exists that adjustments to the turbulence model might have been made simply to offset errors in the numerical scheme, and that these adjustments will prove to have been unnecessary when verification of the second-order version of the method is completed.

The two new models appear to have corrected the lack of responsiveness to adverse pressure gradients leading to separation. Agreement with the two sets of two-dimensional data (Figures 16 through 18) is improved, and the agreement with the swept-wing data is substantially improved (Figures 19 through 21). Model B, in particular, produces approximately the correct variation of crossflow angle through the boundary layer, at Station #7. Both new models produce good agreement with the measured resultant velocity profile, although there is a tendency to underpredict the level of turbulent kinetic energy. As in the case of the flat-plate flow, Model B appears to give the most accurate predictions of wall shear stress.

The proposed modifications have only a minimal effect on the comparison with the swept-shock data (Figures 22 and 23). This observation seems to indicate that the discrepancies between the original model and Peake's experiment were not closely related to the discrepancies between it and the other test cases. The reasons behind the unsatisfactory agreement with the swept-shock data need to be explored more fully, and a more sophisticated calculation performed in which edge boundary conditions can be controlled more precisely. As it stands the comparison does not provide either positive or negative support for the proposed changes to the model.

SECTION V. CONCLUSIONS AND RECOMMENDATIONS

Subject to rather severe constraints imposed on this study by funding limitations, the immediate objectives have been accomplished. The turbulence model, on which the method of Reference 1 is based, has been found to behave well except close to separation. In small and moderate pressure gradients the predicted profiles of velocity and turbulent kinetic energy are in satisfactory agreement with experiment. At low Reynolds numbers and Mach numbers the predicted wall shear stress is within about 5 - 10% of measured values, and the error appears to decrease with increase of either Reynolds number or Mach number. On the other hand, the model exhibits a lack of responsiveness to strong adverse pressure gradients leading to separation, and this weakness seems to be somewhat more serious for three-dimensional flows than for those in two dimensions. For one of the three-dimensional flows studied here: flow over a swept wing, the streamline deflections were underpredicted, and correspondingly, the observed pattern of separation onset was not reflected by the calculation. For the rather extreme case of supersonic flow through a swept shock, the model performed as well as could, perhaps, be expected. Discrepancies with the data were found in this case; however the importance of the discrepancies is difficult to assess because of uncertainties in the measurements and the difficulty of setting up the calculation to reflect appropriate boundary conditions.

Attempts have been made to fine-tune the turbulence model by making a number of modifications and observing the consequent effect on the agreement between theory and experiment. The results are not conclusive, primarily because the optimization involved only a few sets of data, but two alternative new models (represented by particular choices of the empirical functions) are proposed which seem to perform better than the original model.

One of them consists of a modification to the functional relationship between shear stress and turbulent kinetic energy. The other consists of a modification to this same relationship and also a modification to the way in which the dissipation length is represented. In the second model the dissipation length is expressed, as before, as a function of position through the boundary layer, but now relative to a characteristic length which lags behind the local boundary-layer thickness. This lag is intended to reflect the finite response time governing the dynamic relationship between the size of the large eddies and the scale of the turbulent flow.

Implementation of the second of these proposed modifications in the computer code has only been carried out rather crudely, and both modifications involve a weakness regarding invariance to the coordinate system. The shear-stress/turbulent-kinetic-energy relationship corresponds to a generalized constitutive relationship between stress and strain. The form provisionally adopted in the proposed modifications corresponds to a constitutive relationship which does not have the necessary property of invariance. A further modification would be needed to recover this property, and certain associated coding changes would be involved. It is strongly recommended that this additional work be carried out so as to improve the generality of the model.

It is worth mentioning, too, that the study of alternate constitutive relationships would likely be a fruitful area of research in turbulent flows. The limitations of isotropic eddy-viscosity models (even those, like the model of Reference 1, in which the magnitude of the eddy viscosity is not prescribed in advance) are well known. But little has been done to remedy their deficiencies other than certain attempts to calculate all the elements of the Reynolds stress tensor separately. Such an approach introduces even more uncertainties, and it may be preferable, insteady, to represent the stress tensor in terms of a smaller number of independent variables together with an appropriate constitutive relationship for generating the individual elements. It is rapidly becoming apparent that the normal stresses can not be ignored if the model is to have general validity, and a sound, economical means of dealing with the complete tensor is urgently needed.

Another urgent extension of this study would consist of testing the proposed modifications to the model in a second-order-accurate version of the calculation method. This step is necessary to check whether the modifications actually represent improvements in the turbulence model, or represent nothing more than devices for generating additional errors to offset those associated with the numerical scheme.

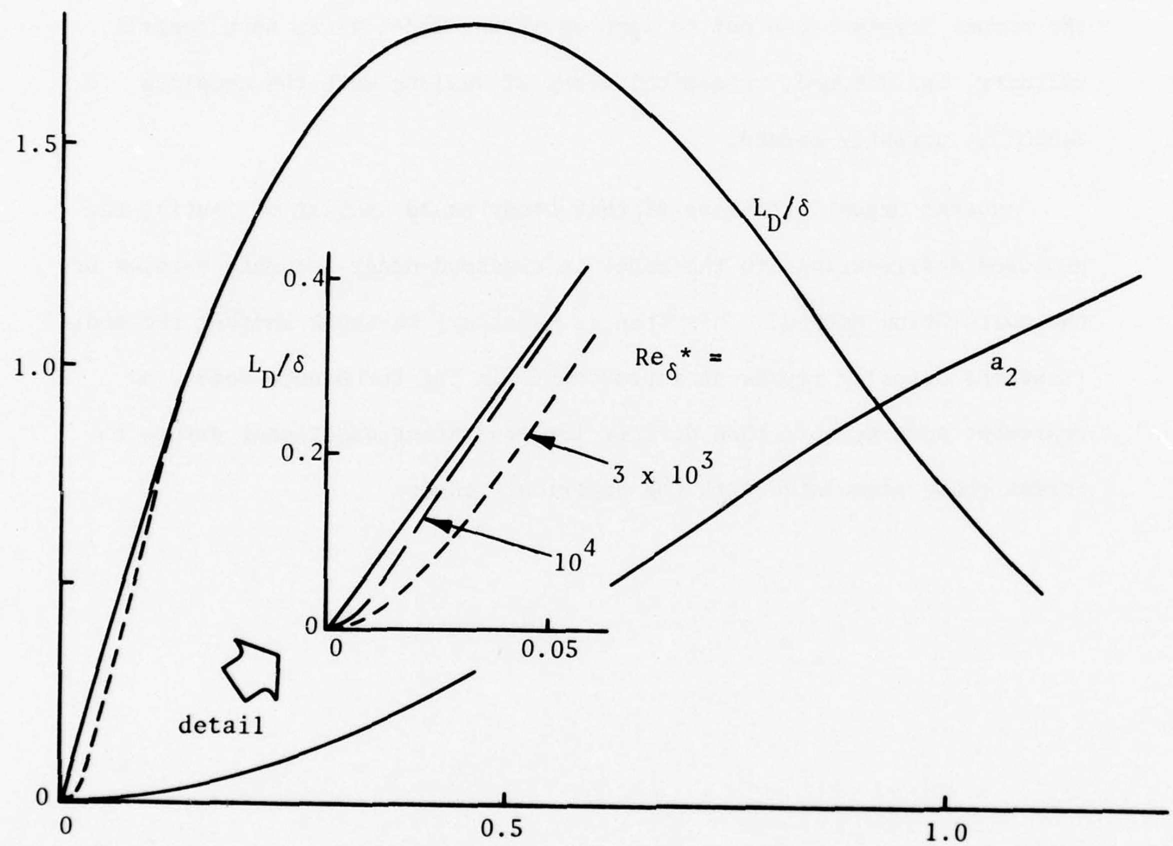

FIGURE 1 DIFFUSION FUNCTION AND DISSIPATION LENGTH

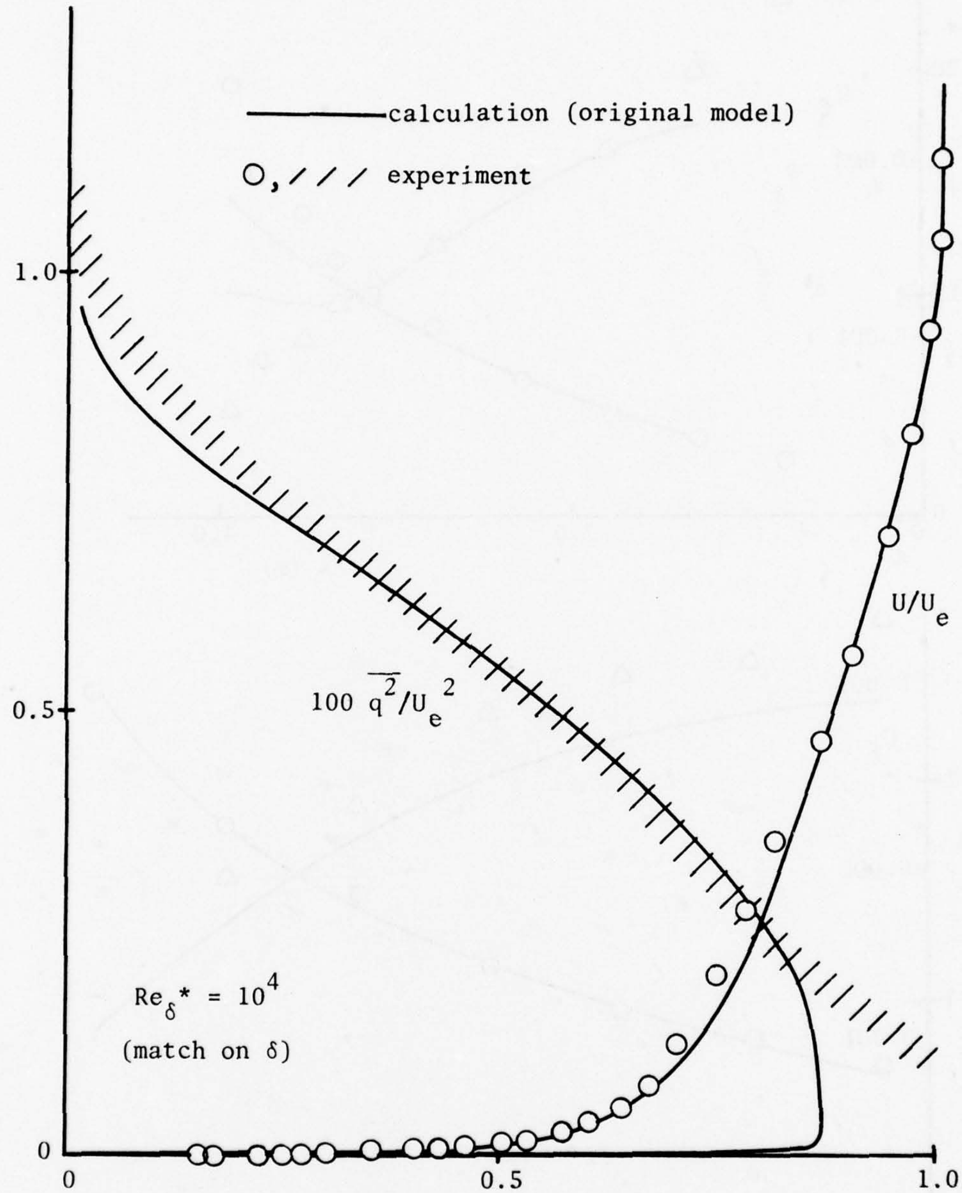

FIGURE 2 COMPARISON WITH THE DATA OF KLEBANOFF (VELOCITY AND $\overline{q^2}$ PROFILES)

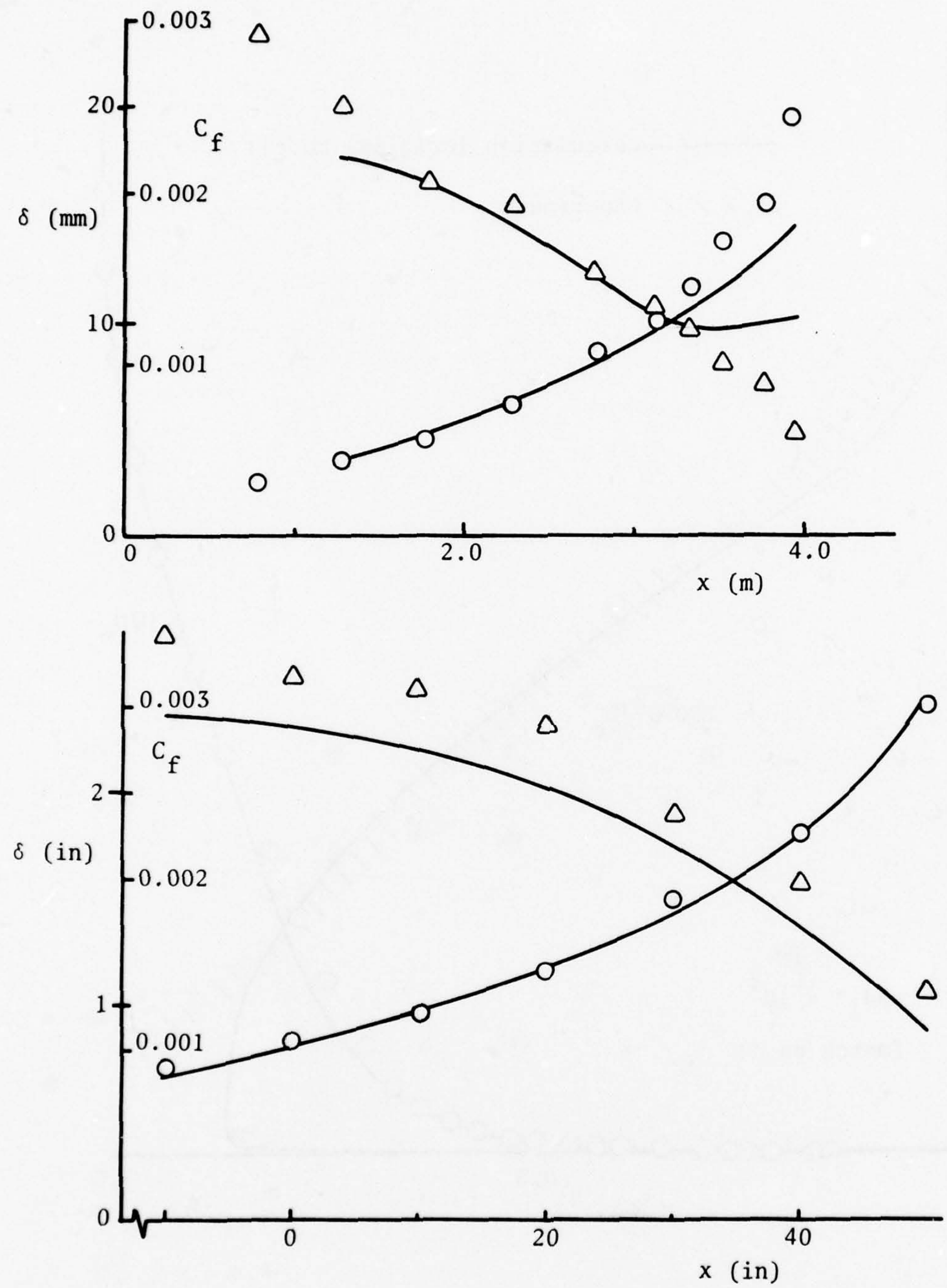

FIGURE 3 COMPARISON WITH THE DATA OF LUDWIEG AND TILLMANN, AND SCHUBAUER AND SPANGENBERG (WALL SHEAR STRESS AND BOUNDARY-LAYER THICKNESS)

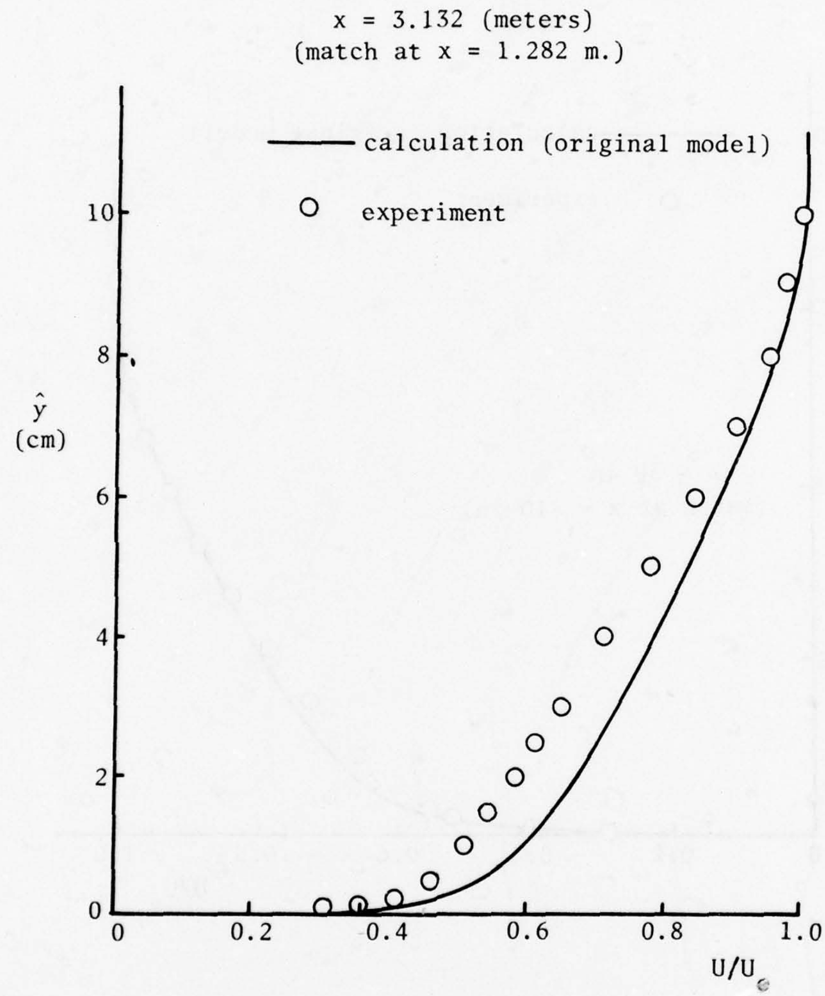

FIGURE 4 COMPARISON WITH THE DATA OF LUDWIEG AND TILLMANN (VELOCITY PROFILE)

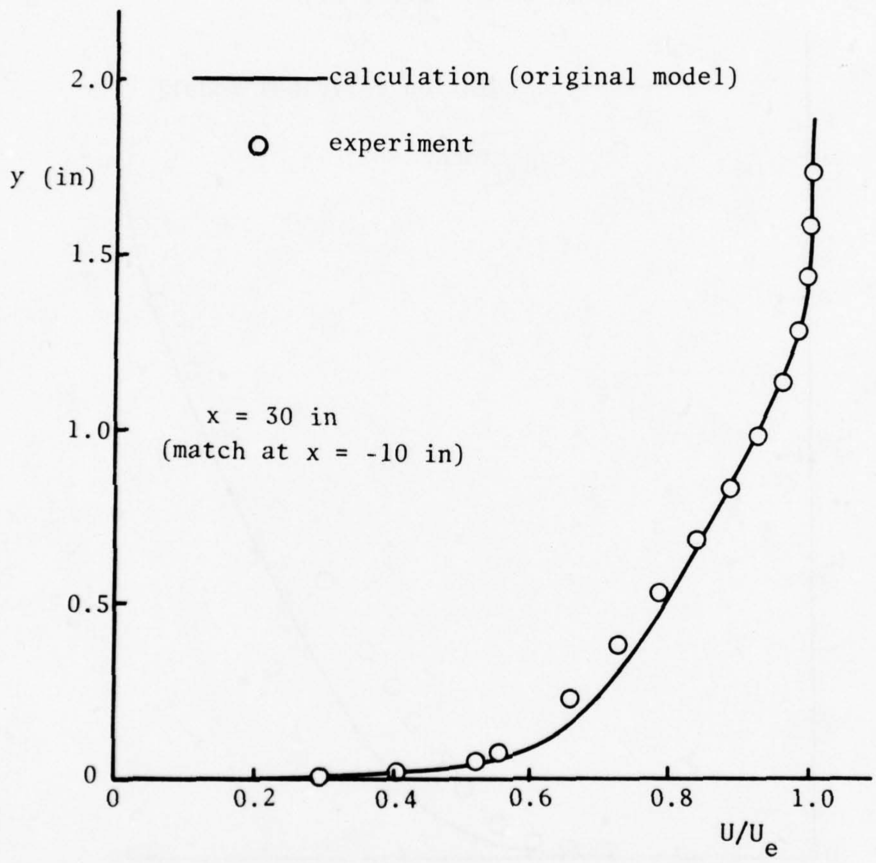

FIGURE 5 COMPARISON WITH THE DATA OF SCHUBAUER AND SPANGENBERG (VELOCITY PROFILE)

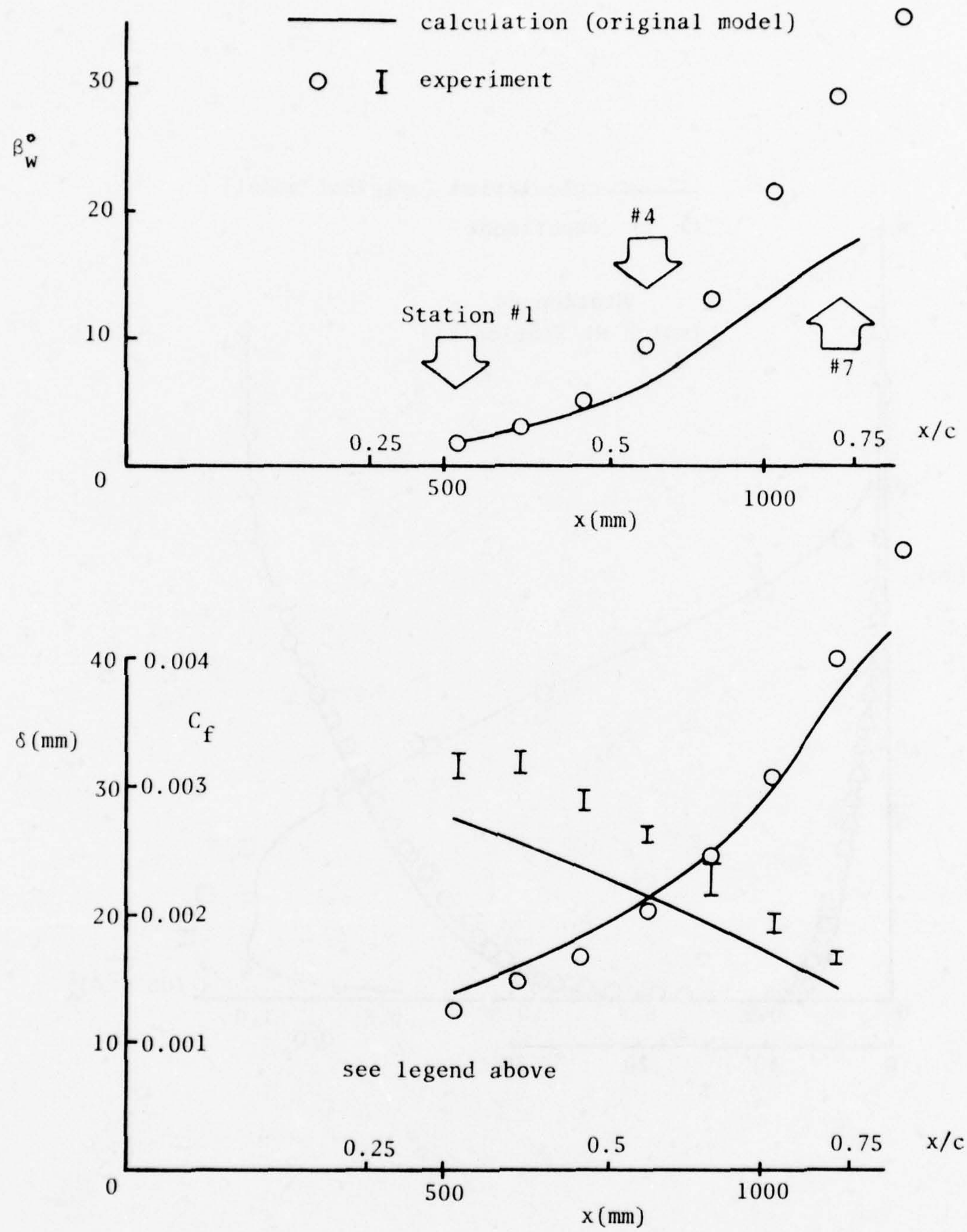

FIGURE 6 COMPARISON WITH THE DATA OF VAN DEN BERG AND ELSENAAR (WALL SHEAR STRESS AND BOUNDARY-LAYER THICKNESS)

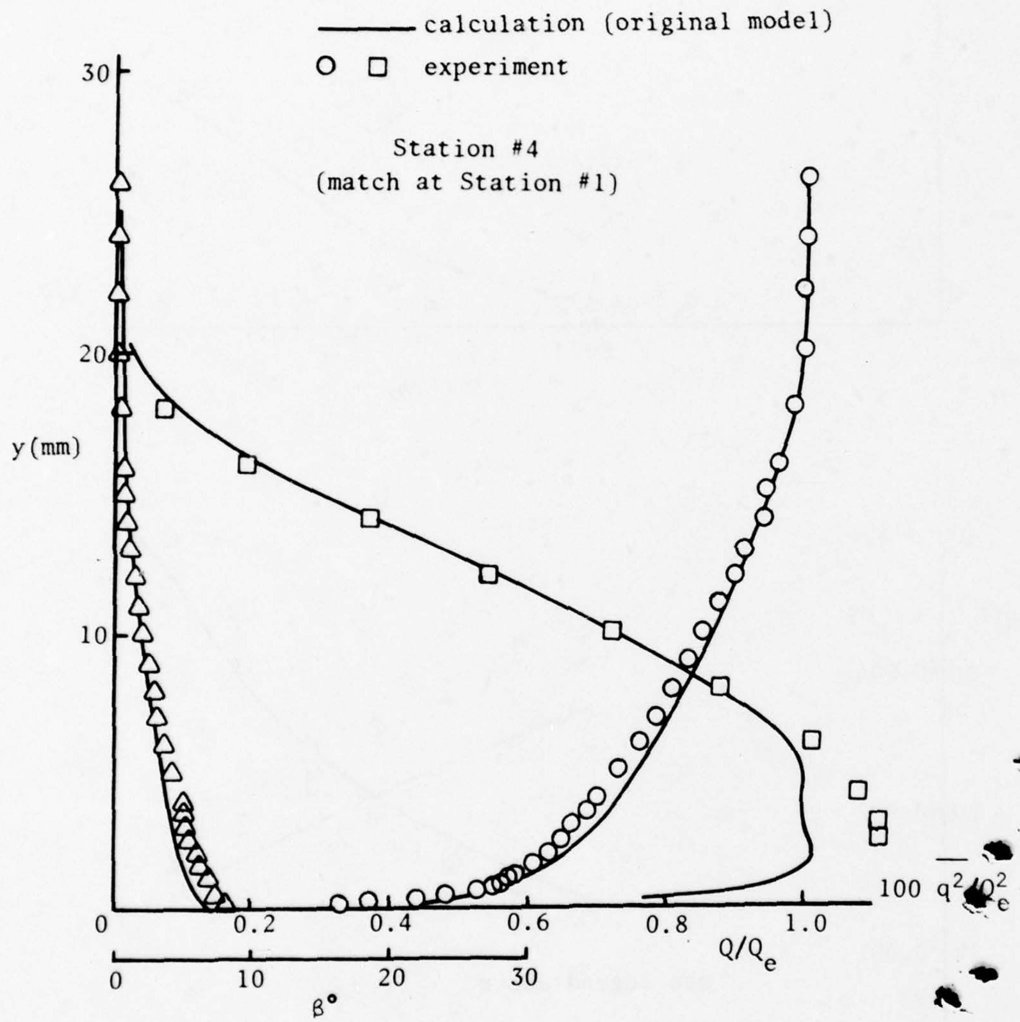

FIGURE 7 COMPARISON WITH THE DATA OF VAN DEN BERG AND ELSENAAR (VELOCITY AND $\overline{q^2}$ PROFILES AT STATION #4)

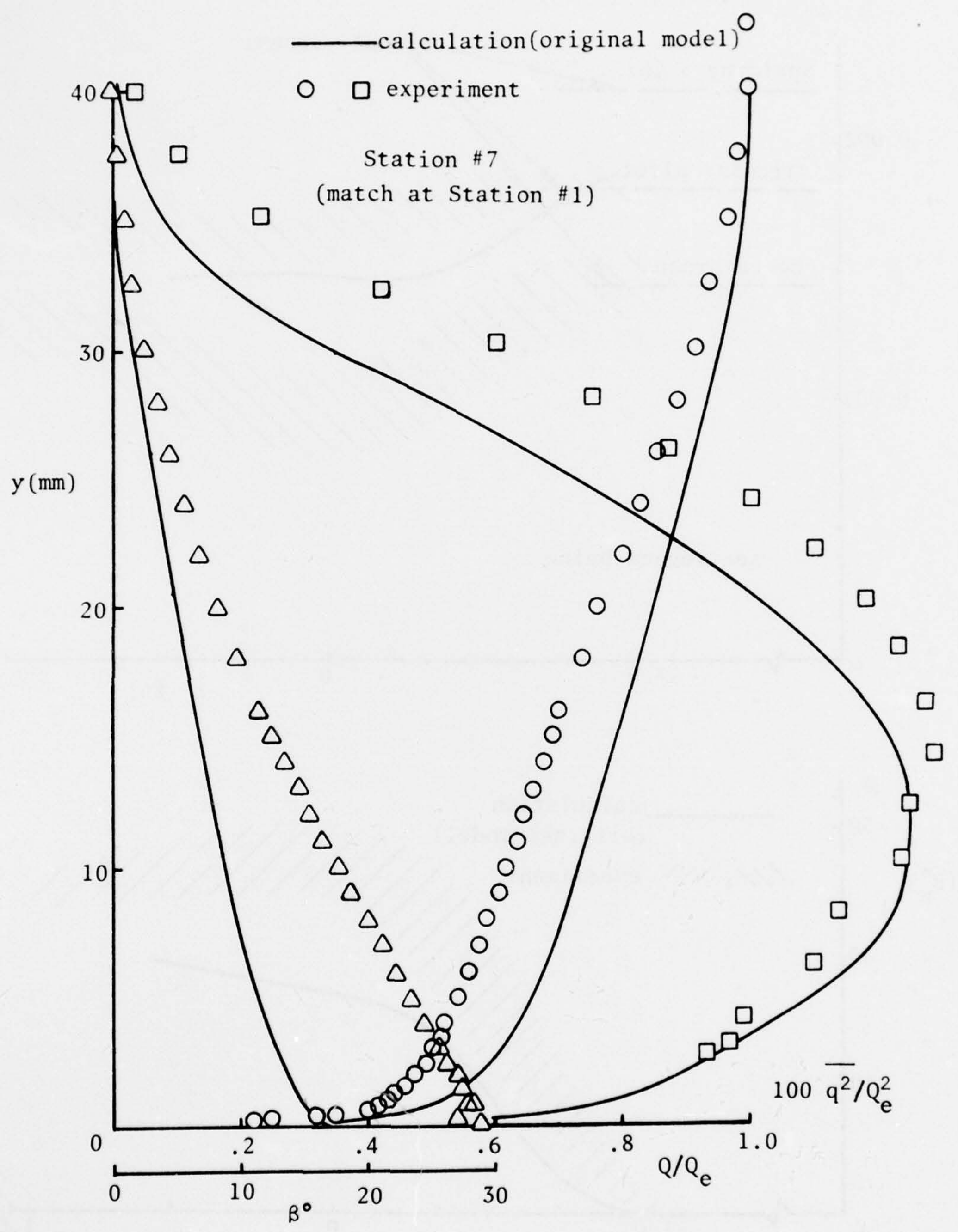

FIGURE 8 COMPARISON WITH THE DATA OF VAN DEN BERG AND ELSENAAR (VELOCITY AND $\overline{q^2}$ PROFILES AT STATION #7)

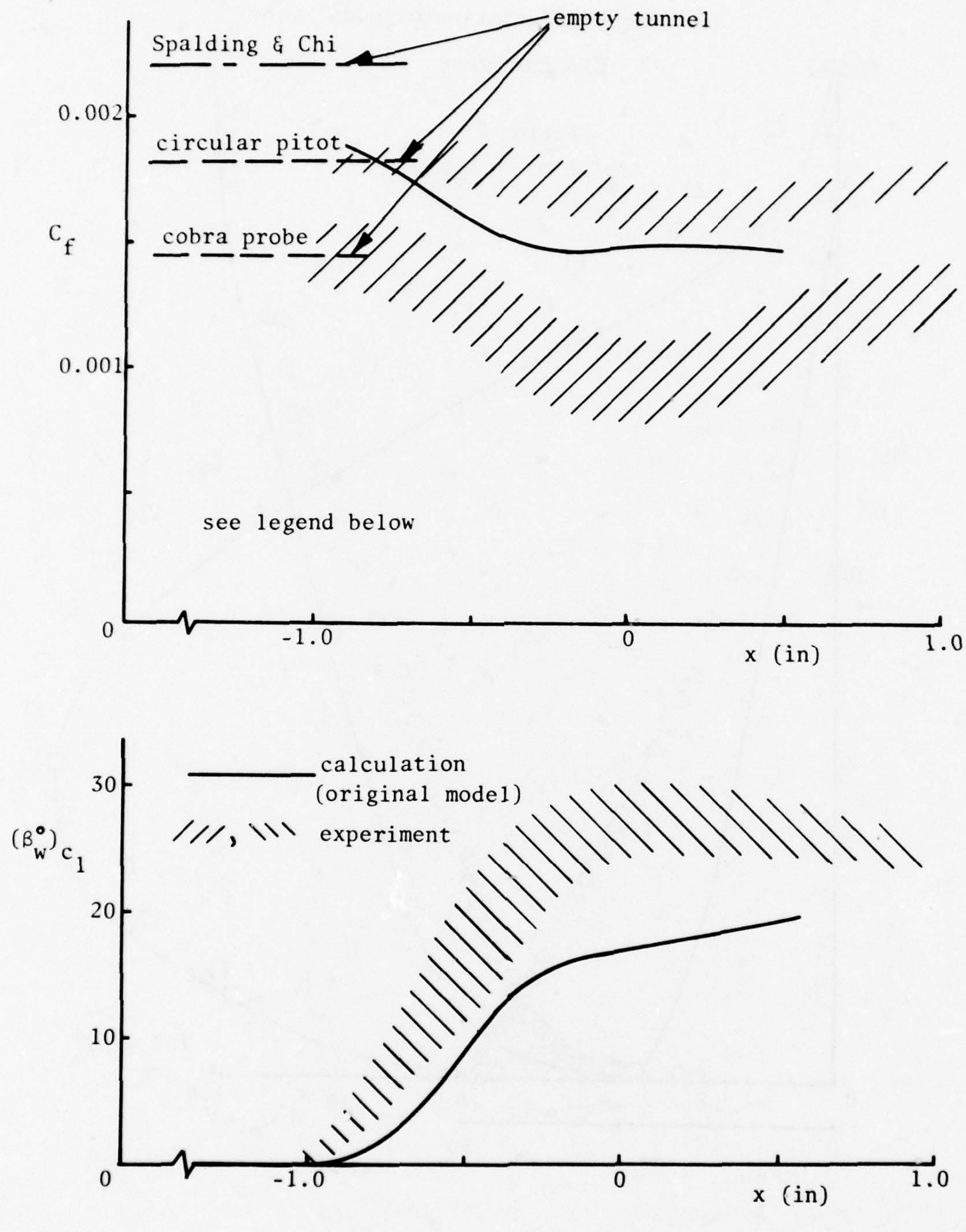

FIGURE 9 COMPARISON WITH THE DATA OF PEAKE
(WALL SHEAR STRESS)

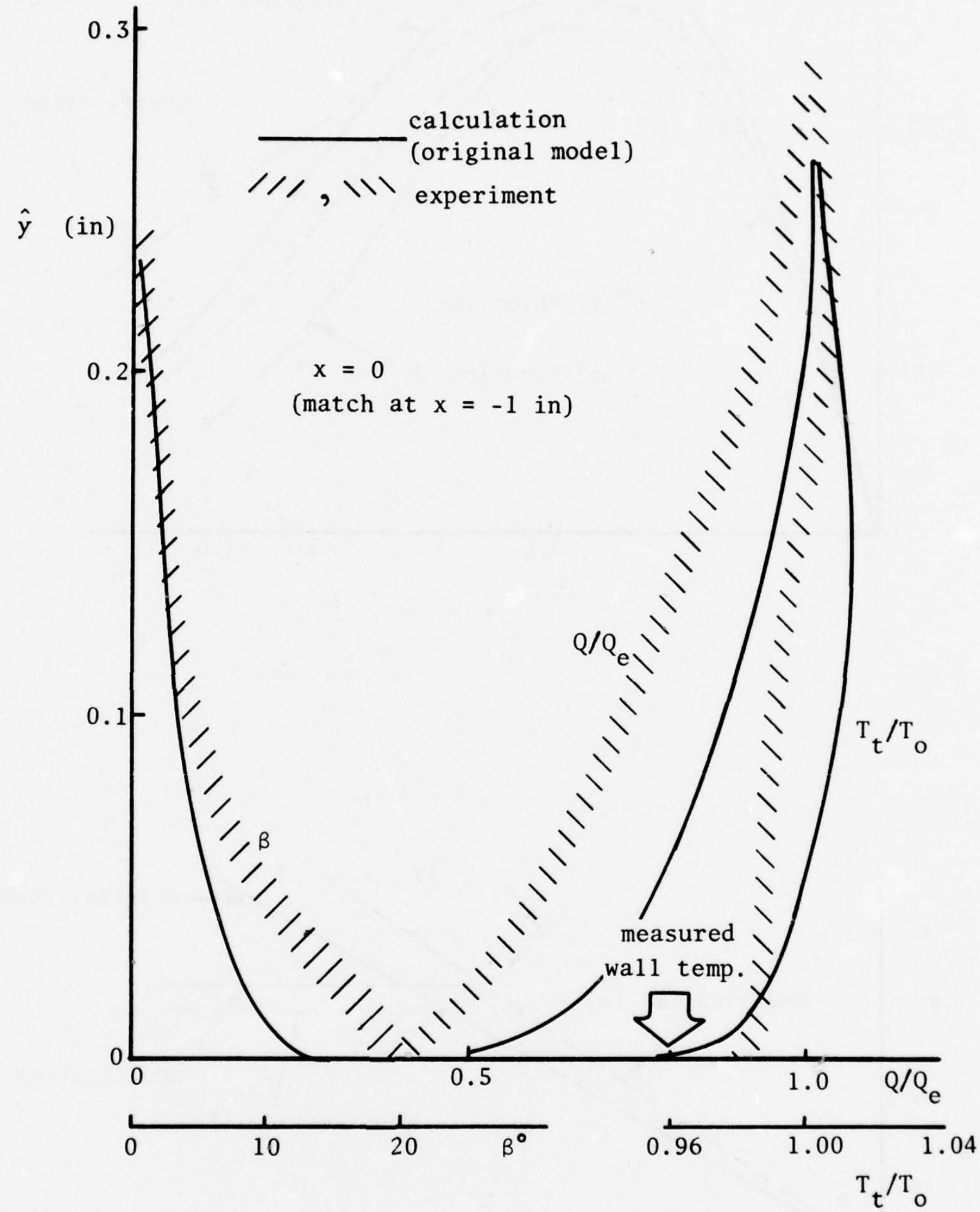

FIGURE 10 COMPARISON WITH THE DATA OF PEAKE (VELOCITY AND TEMPERATURE PROFILES)

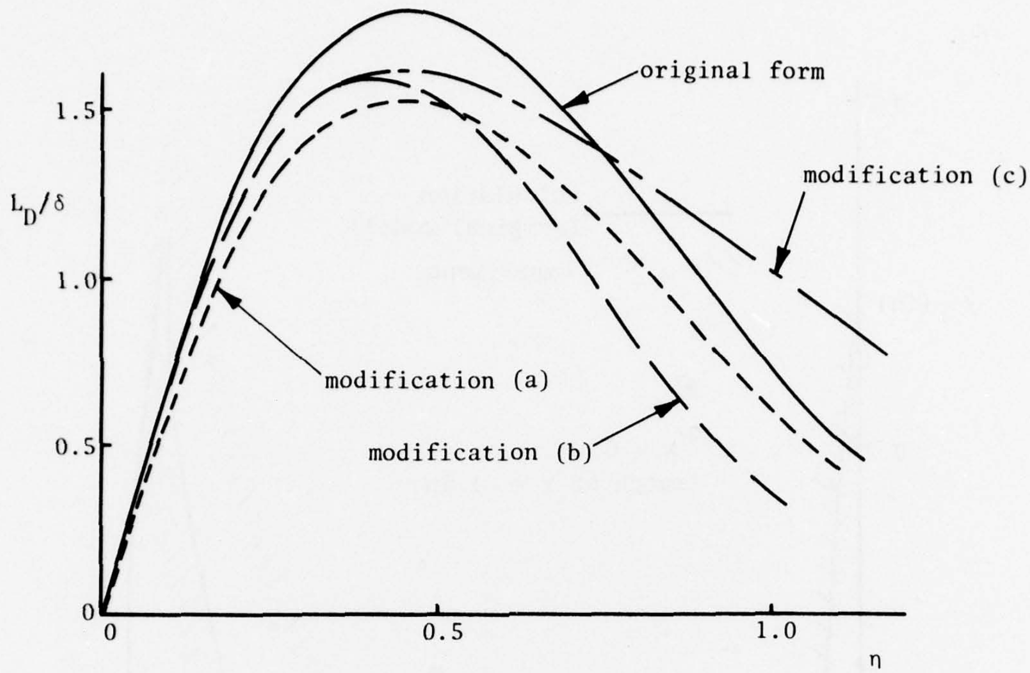

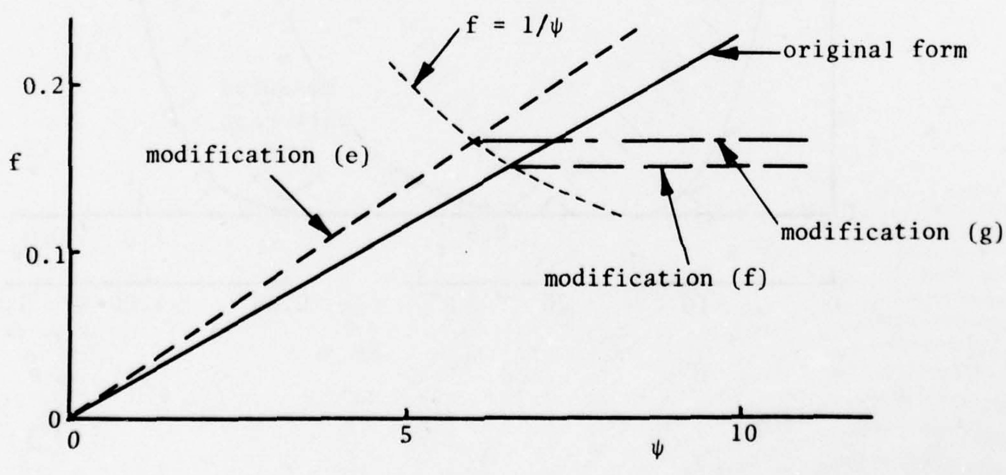

FIGURE 11 MODIFICATIONS TO DISSIPATION LENGTH AND f(ψ) CONSIDERED IN THE SENSITIVITY STUDY

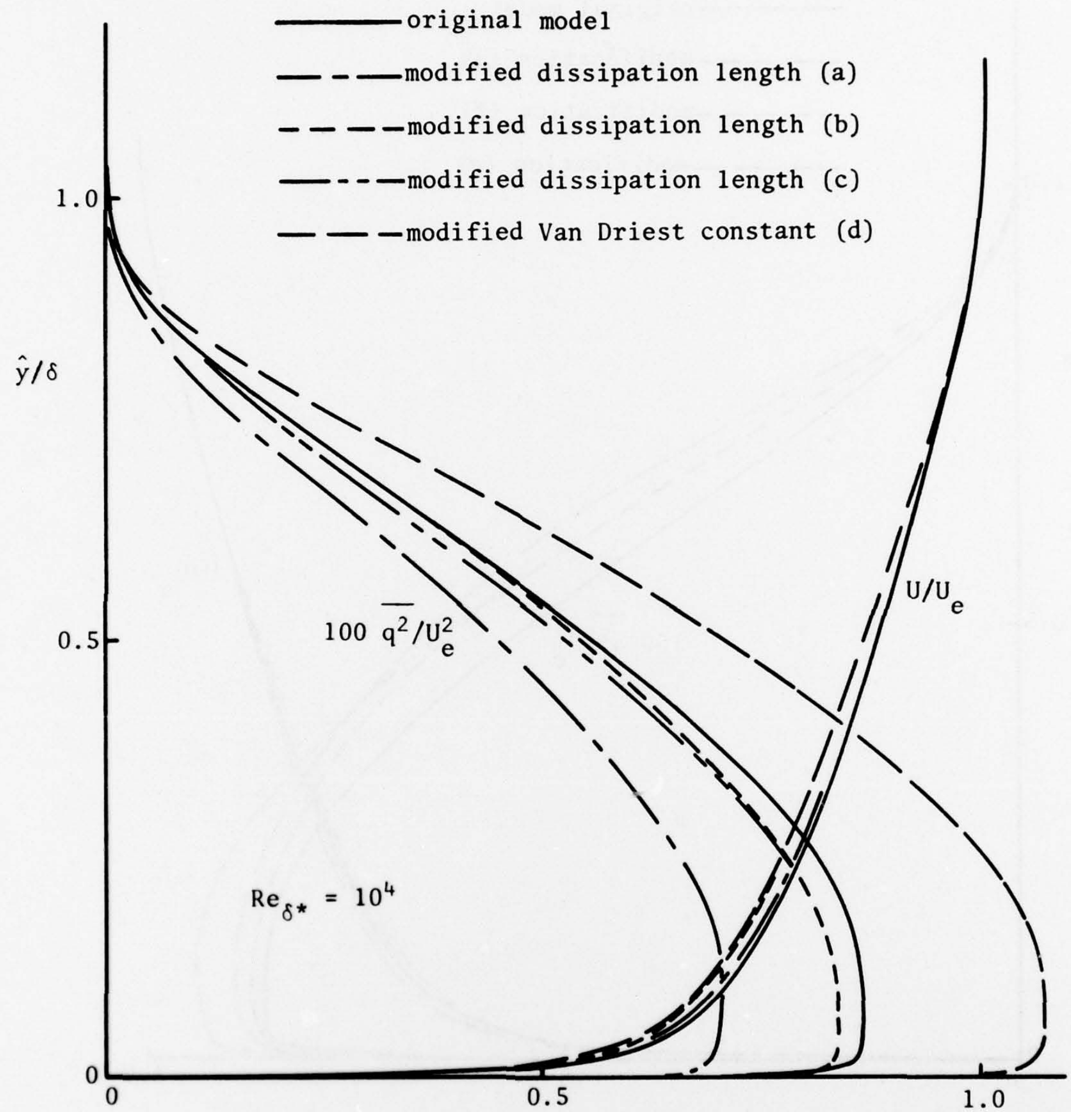

FIGURE 12 EFFECT OF MODIFICATIONS TO DISSIPATION LENGTH

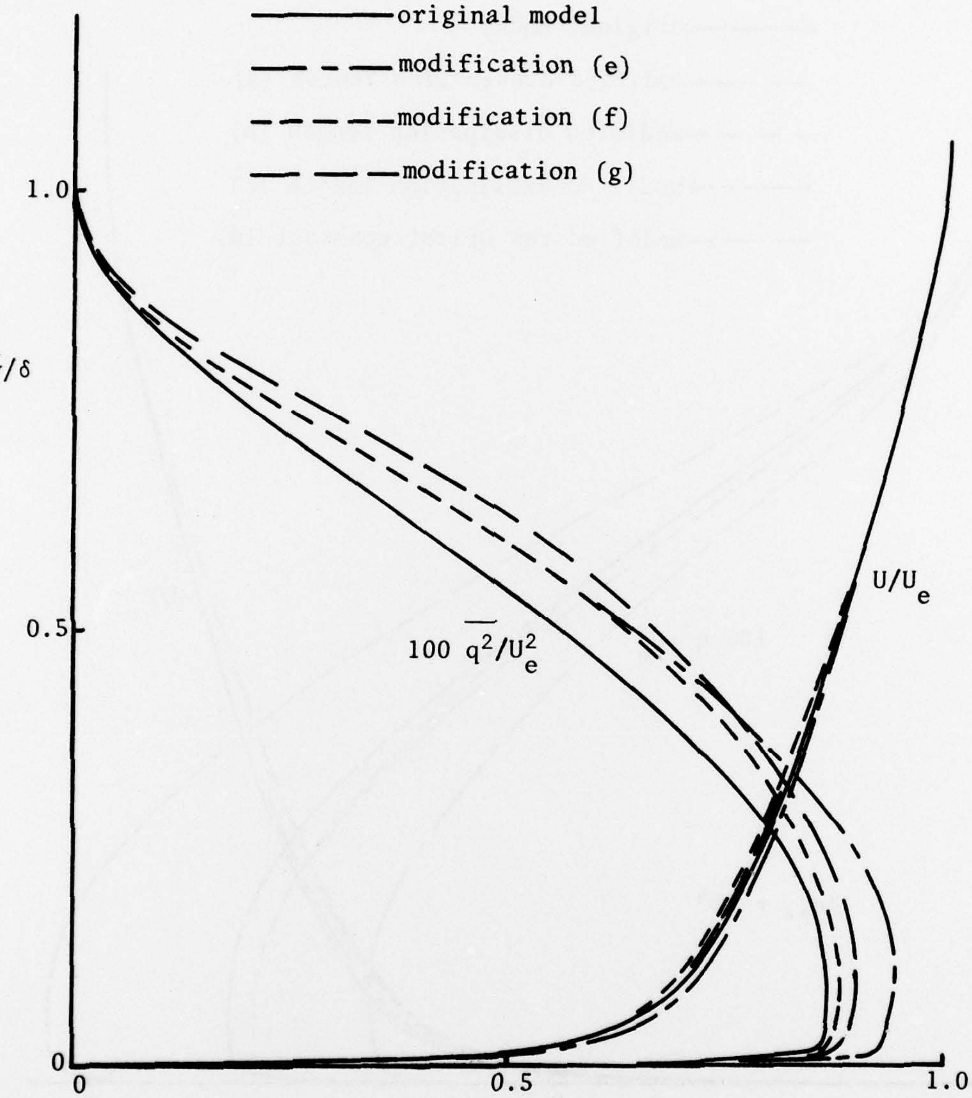

FIGURE 13 EFFECT OF MODIFICATIONS TO THE SHEAR-STRESS/ TURBULENT-KINETIC-ENERGY RELATIONSHIP

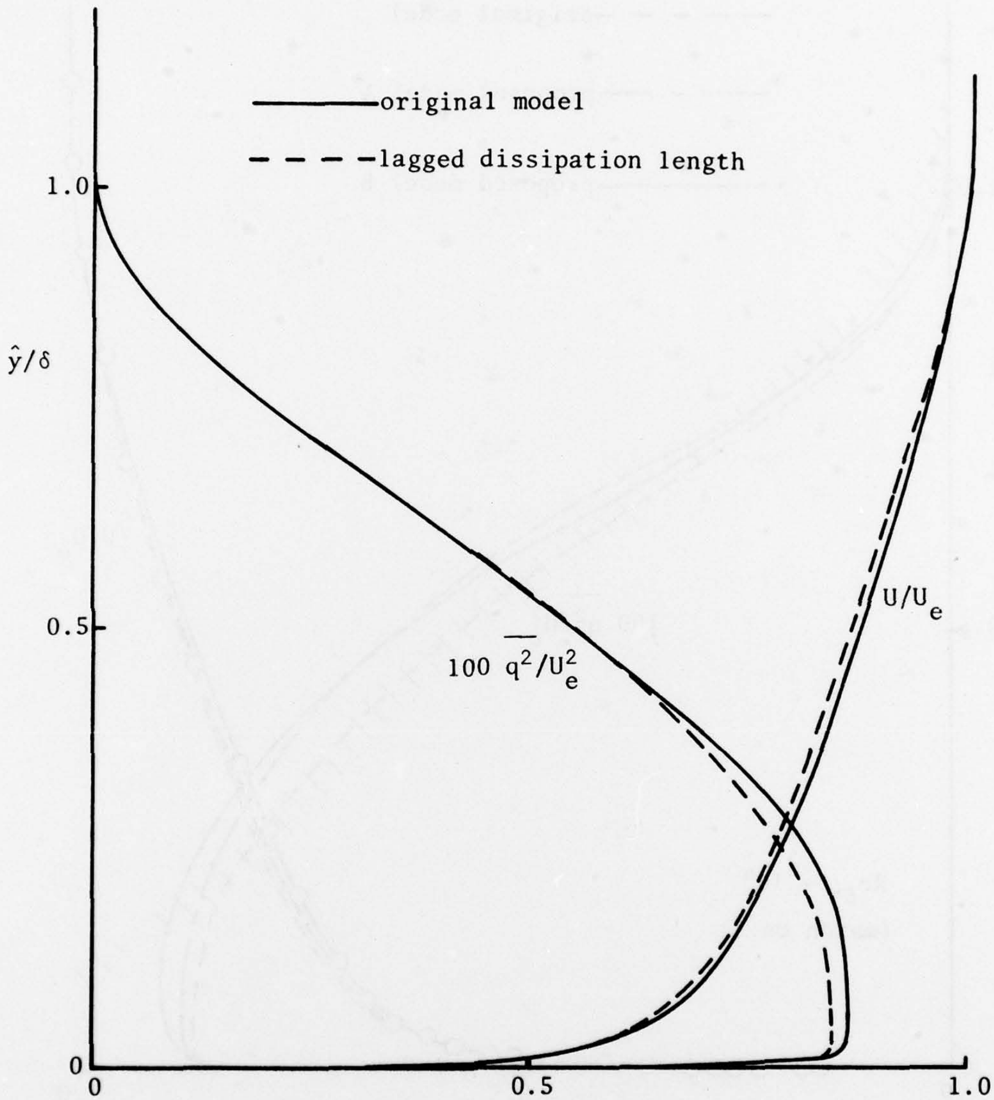

FIGURE 14 EFFECT OF REPRESENTING THE FINITE RESPONSE TIME OF THE DISSIPATION LENGTH

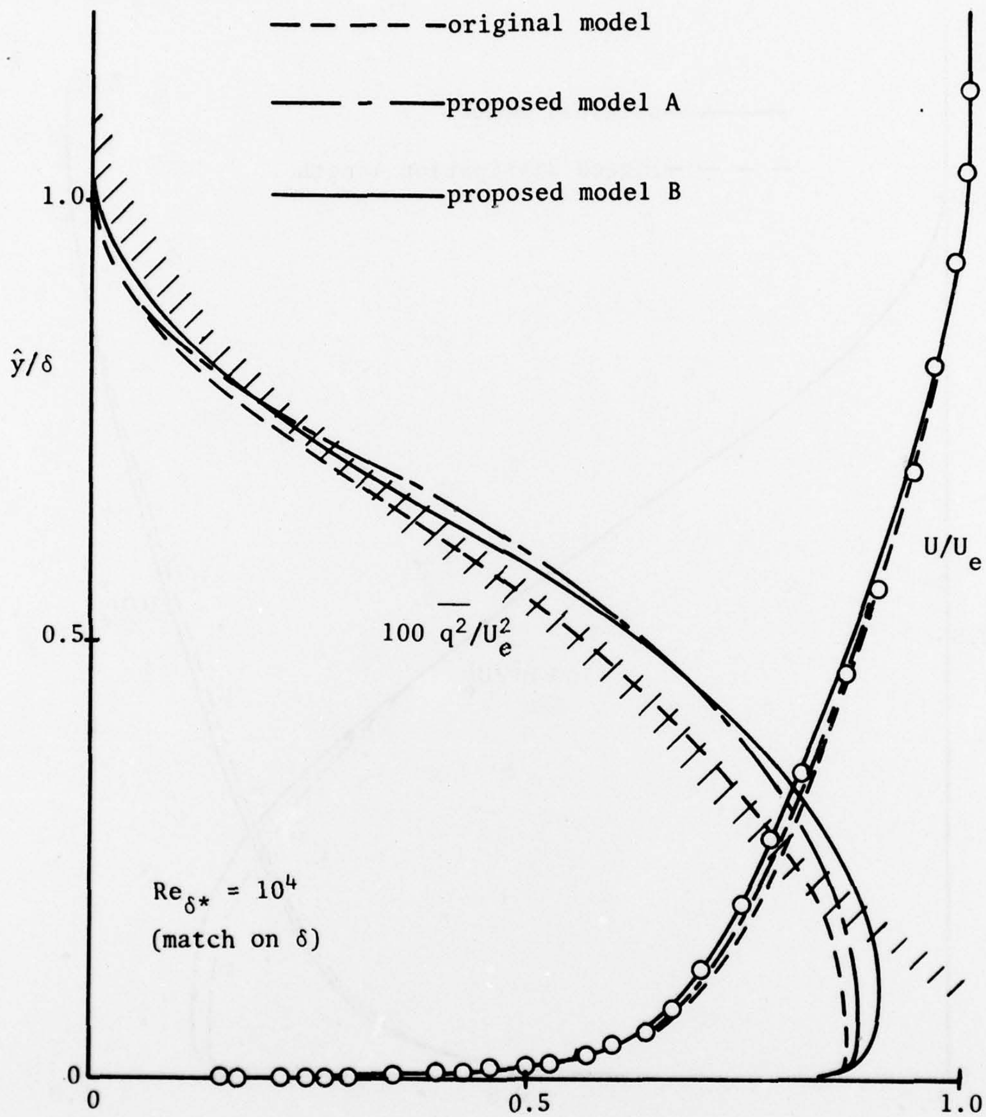

FIGURE 15 COMPARISON WITH THE DATA OF KLEBANOFF
(VELOCITY AND $\overline{q^2}$ PROFILES)

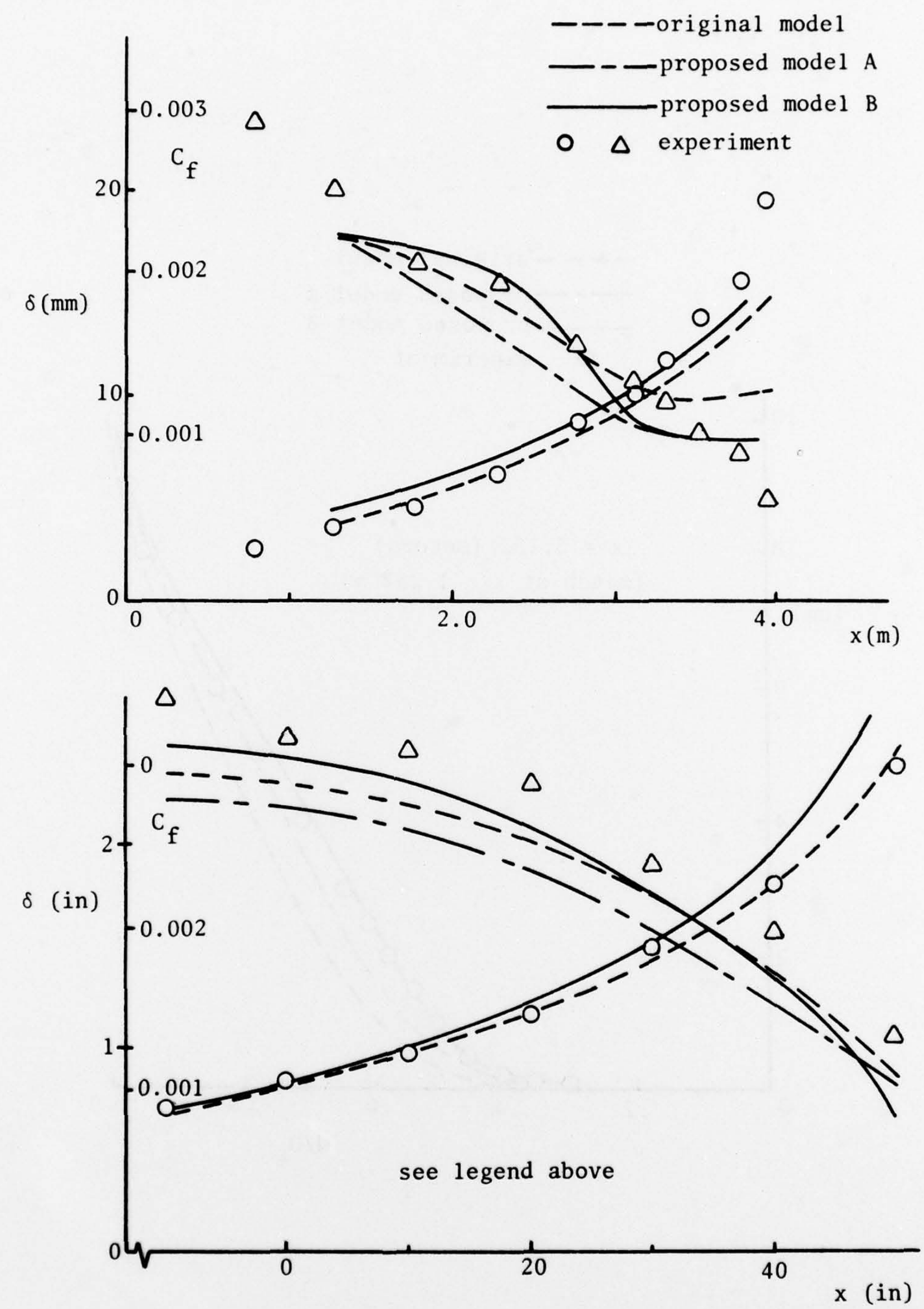

FIGURE 16 COMPARISON WITH THE DATA OF LUDWIEG AND TILLMANN, AND SCHUBAUER AND SPANGENBERG (WALL SHEAR STRESS AND BOUNDARY-LAYER THICKNESS)

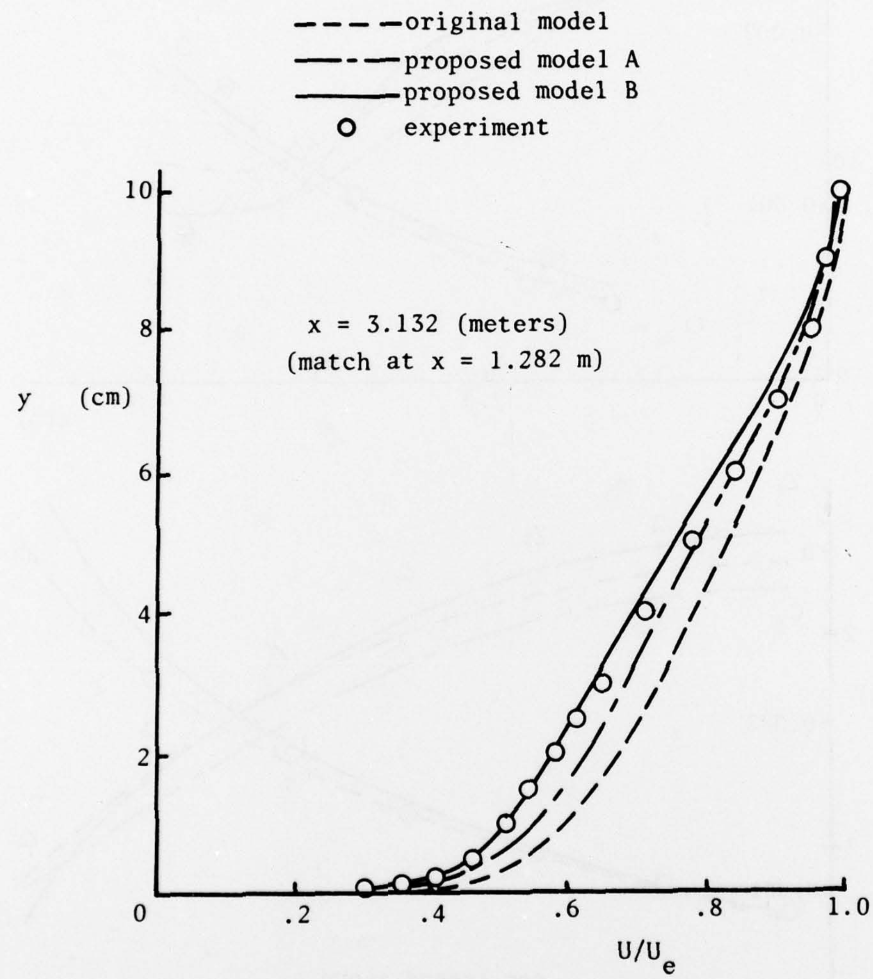

FIGURE 17 COMPARISON WITH THE DATA OF LUDWIEG AND TILLMANN (VELOCITY PROFILE)

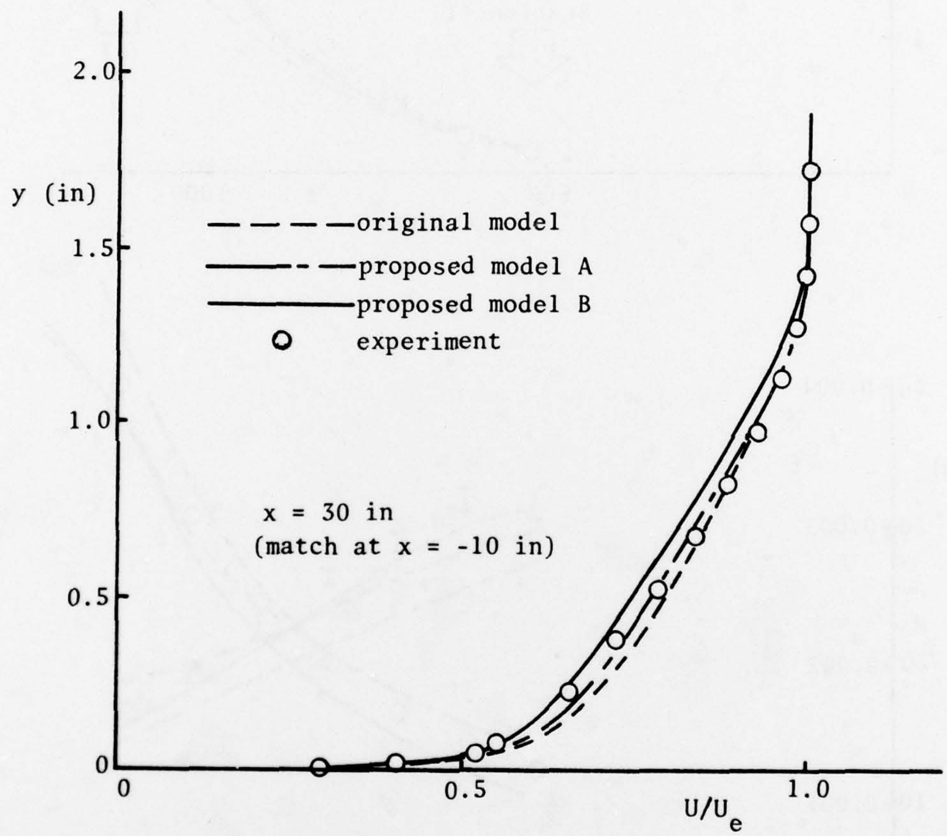

FIGURE 18 COMPARISON WITH THE DATA OF SCHUBAUER AND SPANGENBERG (VELOCITY PROFILE)

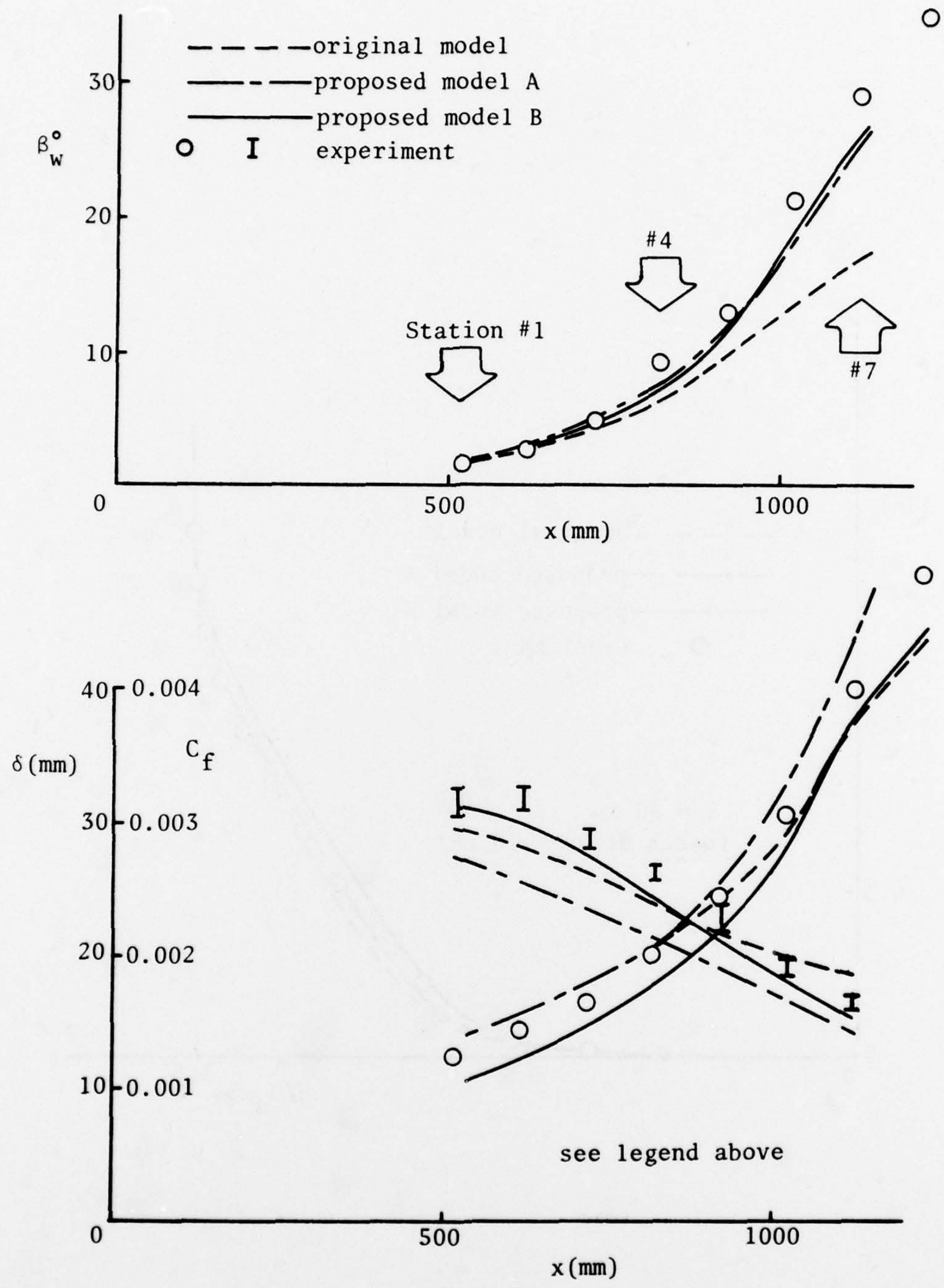

FIGURE 19 COMPARISON WITH THE DATA OF VAN DEN BERG AND ELSENAAR (WALL SHEAR STRESS AND BOUNDARY-LAYER THICKNESS)

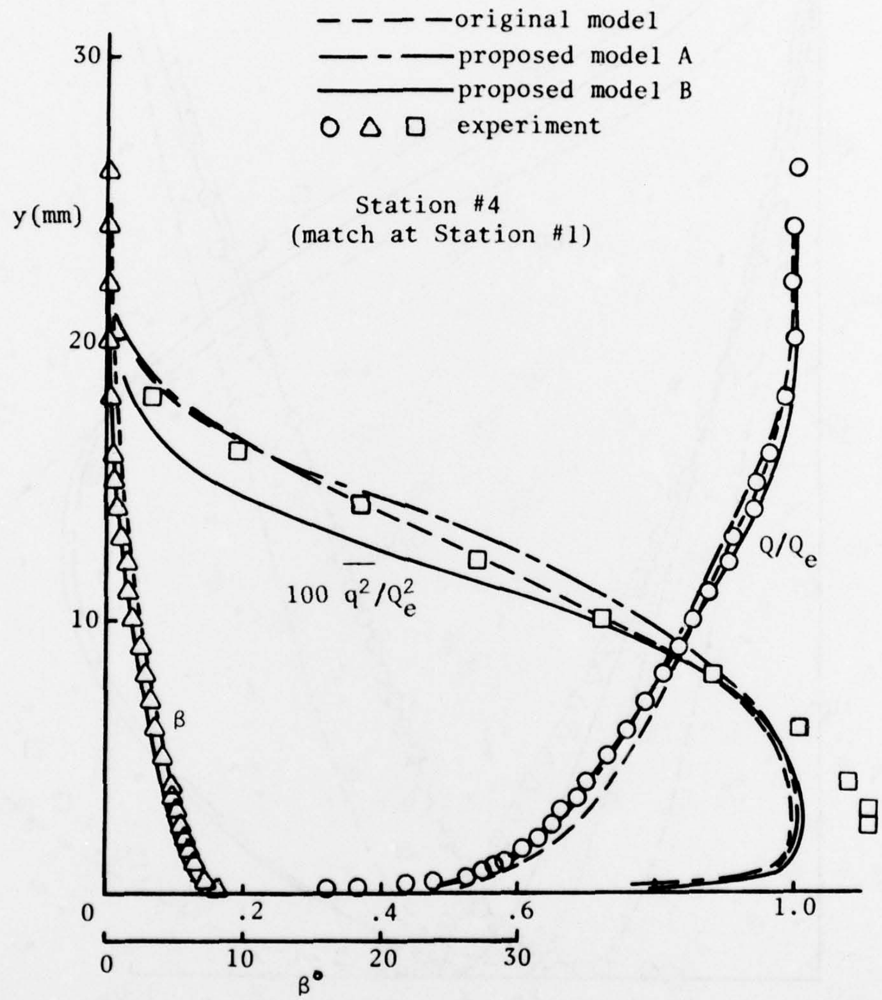

FIGURE 20 COMPARISON WITH THE DATA OF VAN DEN BERG AND ELSENAAR (VELOCITY AND $\overline{q^2}$ PROFILES AT STATION #4)

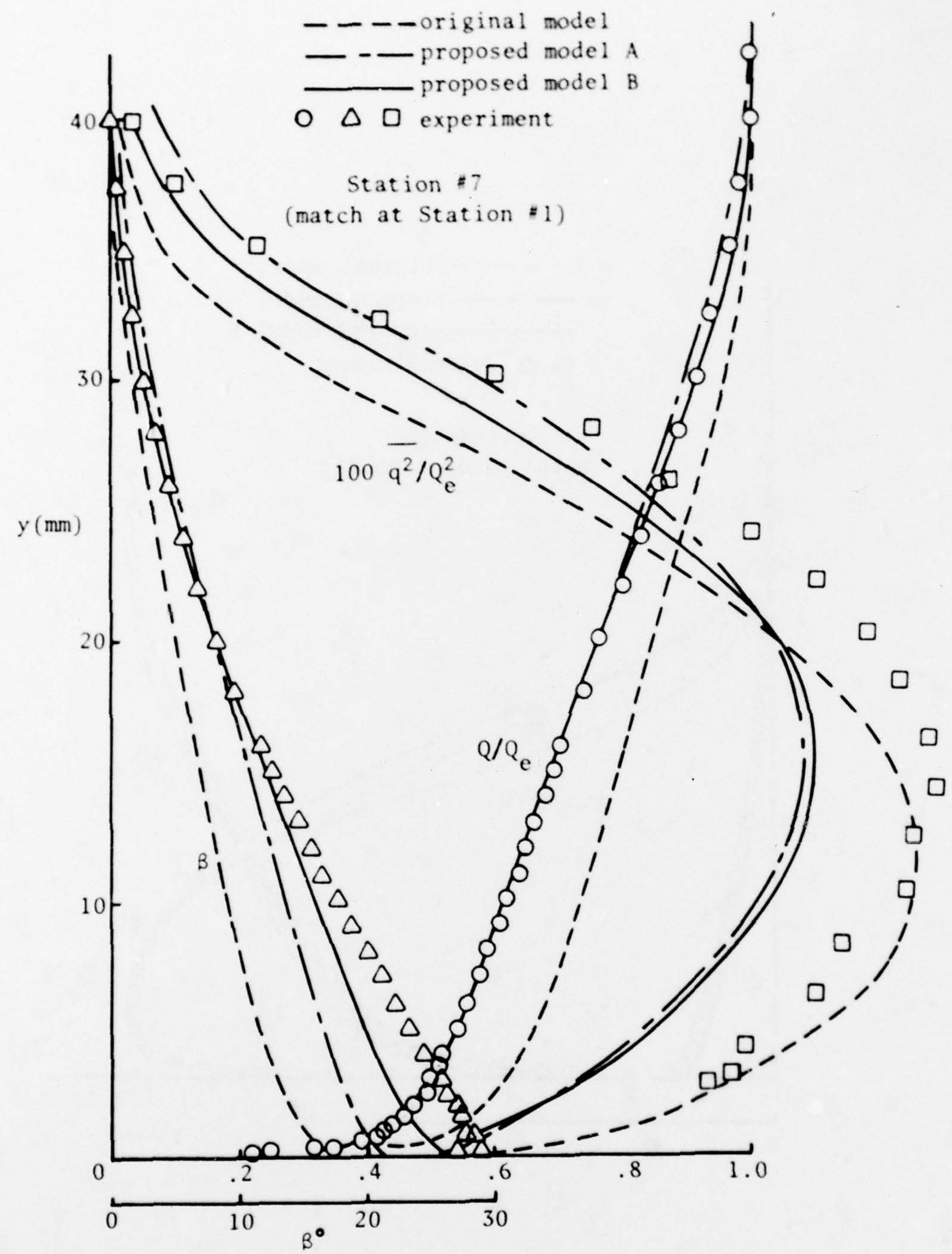

FIGURE 21 COMPARISON WITH THE DATA OF VAN DEN BERG AND ELSENAAR (VELOCITY AND $\overline{q^2}$ PROFILES AT STATION #7)

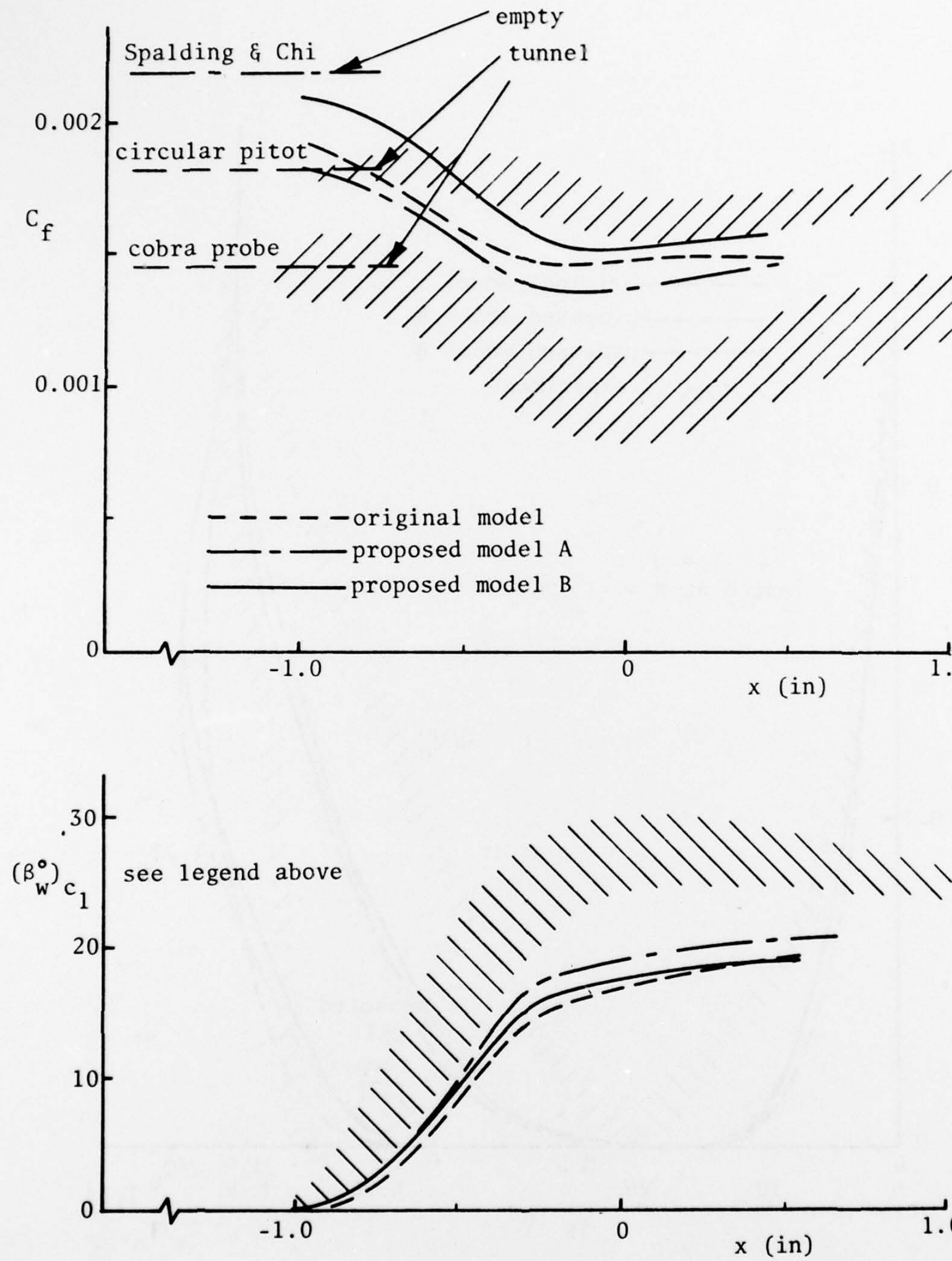

FIGURE 22 COMPARISON WITH THE DATA OF PEAKE (WALL SHEAR STRESS)

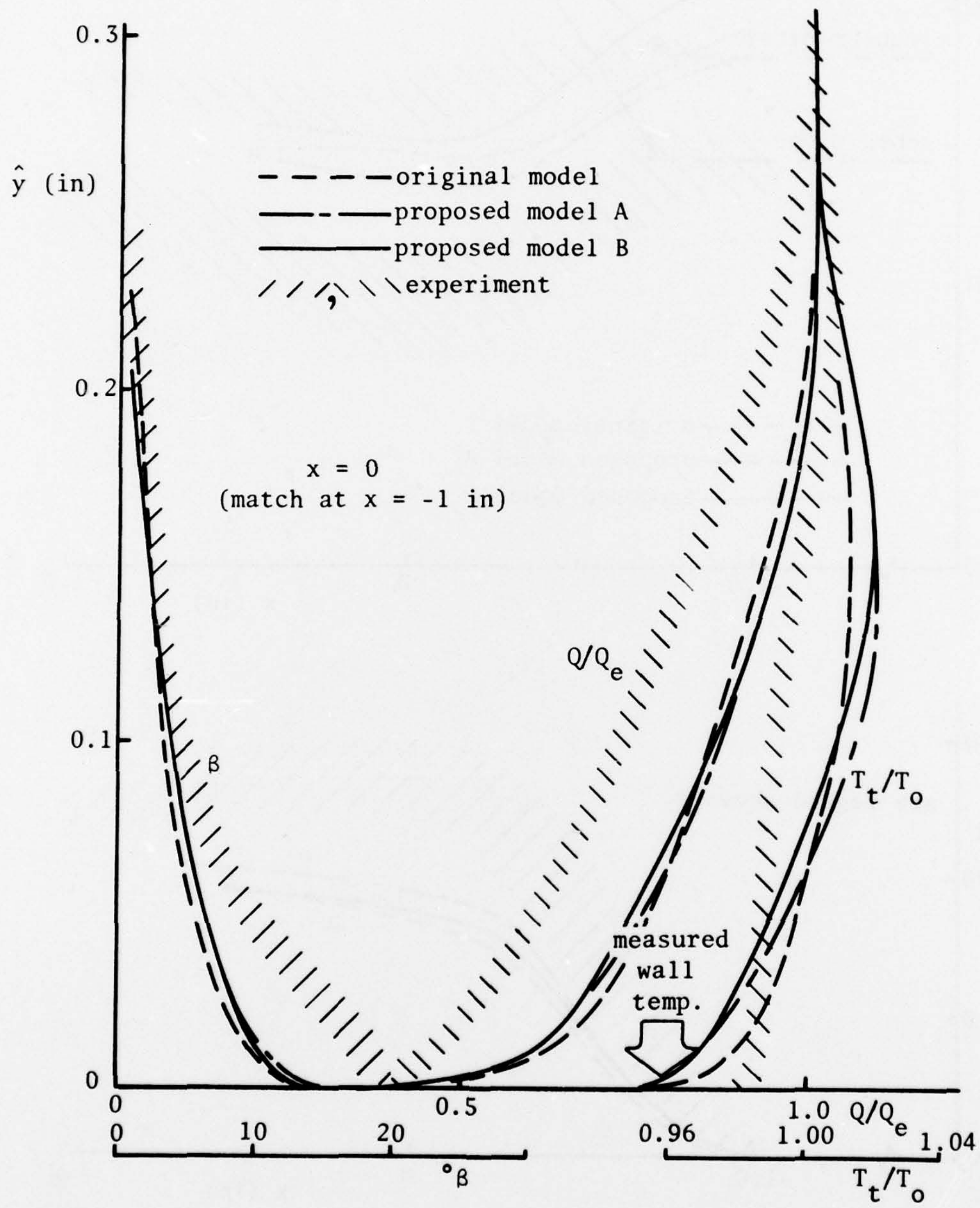

FIGURE 23 COMPARISON WITH THE DATA OF PEAKE (VELOCITY AND TEMPERATURE PROFILES)

REFERENCES

1. Nash, J. F., and Scruggs, R. M., "An Implicit Method for the Calculation of Three-Dimensional Boundary Layers on Finite, Thick Wings", Sybucon Report SYB-76-002, August 1976, Air Force Contract F33615-75-C-3073.

2. Nash, J.F., "Three-Dimensional Turbulent Boundary Layers in Incompressible Flow", J. Fluid Mech. 37, part 4, p.625, 1969.

3. Bradshaw, P., Ferriss, D.H., and Atwell, N.P., "Calculation of Boundary-Layer Development Using the Turbulent Energy Equation", J. Fluid Mech. 28, part 3, p. 593, 1967.

4. Nash, J. F., and Patel, V. C., "A Generalization Method for the Calculation of Three-Dimensional Turbulent Boundary Layers", Project SQUID Symposium, Georgia Institute of Technology, 1971.

5. Nash, J. F., and Patel, V. C., Three-Dimensional Turbulent Boundary Layers, SBC Technical Books, 1972.

6. Van Driest, E. R., "On Turbulent Flow Near a Wall", J. Aero. Sci. 23, p. 1007, 1956.

7. Klebanoff, P. S., "Characteristics of Turbulence in a Boundary Layer with Zero Pressure Gradient", N.A.C.A. Rep. No. 1247, 1955.

8. Smith, S. W., and Walker, J. H., "Skin-Friction Measurements in Incompressible Flow", NASA TR R-26, 1959.

9. Rotta, J. C., "Turbulent Boundary Layers in Incompressible Flow", Progress in Aeronautical Science, Pergamon Press, 1962.

10. Coles, D., "The Law of the Wall in Turbulent Shear Flow", 50 Jahre Grenzschichtforschung, Vieweg & Sohn, 1955.

11. Ludwieg, H., and Tillmann, W., "Investigations of the Wall Shearing Stress in Turbulent Boundary Layers", Ing.-Arch. 17, p.288, 1949; also NACA TM 1285, 1950.

12. Schubauer, G.B., and Spangenberg, W. G., "Forced Mixing in Boundary Layers", J. Fluid Mech., 8, p. 10, 1960.

13. Coles, D. E., and Hirst, E. A., "Computation of Turbulent Boundary Layers -- 1968 AFOSR-IFP-Stanford Conference; Vol. II: Compiled Data", Dept. of Mech. Eng., Stanford University, 1968.

14. Van den Berg, B., and Elsenaar, A., "Measurements in a Three-Dimensional Incompressible Turbulent Boundary Layer in an Adverse Pressure Gradient Under Infinite Swept Wing Conditions", NLR Report TR 72092 U, 1972.

15. Elsenaar, A., and Boelsma, S. H., "Measurements of the Reynolds Stress Tensor in a Three-Dimensional Turbulent Boundary Layer Under Infinite Swept Wing Condition", NLR Reprot TR 74095 U, 1974.

16. East, L. F., "Computation of Three-Dimensional Turbulent Boundary Layers; Euromech 60, Trondheim 1975", FFA REport TN AE-1211, 1975.

17. Batchelor, G. K., and Proudman, I., "The Effect of Rapid Distortion of a Fluid in Turbulent Motion", Quart. J. Mech. Appl. Mech., 7, p. 83, 1954.

18. Bradshaw, P., and Unsworth, K., "Computations of Complex Turbulent Flows", Reviews in Viscous Flow, (Ed., V. C. Patel), Lockheed-Georgia Co., June 1976.

19. Spalding, D. B., and Chi, S. W., "The Drag of a Compressible Turbulent Boundary Layer on a Smooth Flat Plate with and without Heat Transfer", J. Fluid Mech., 18, p. 117, 1964.

☆U.S.Government Printing Office: 1978 — 757-080/571